

10-2005

# Evaluation of the Use of Lithium Compounds in Controlling Alkali-Silica Reactivity in Concrete Pavement

Christopher Y. Tuan  
*University of Nebraska-Lincoln, ctuan1@unl.edu*

Michael T. Kelly

Mark E. Buss

Follow this and additional works at: <http://digitalcommons.unl.edu/ndor>

 Part of the [Transportation Engineering Commons](#)

---

Tuan, Christopher Y.; Kelly, Michael T.; and Buss, Mark E., "Evaluation of the Use of Lithium Compounds in Controlling Alkali-Silica Reactivity in Concrete Pavement" (2005). *Nebraska Department of Transportation Research Reports*. 2.  
<http://digitalcommons.unl.edu/ndor/2>

This Article is brought to you for free and open access by the Nebraska LTAP at DigitalCommons@University of Nebraska - Lincoln. It has been accepted for inclusion in Nebraska Department of Transportation Research Reports by an authorized administrator of DigitalCommons@University of Nebraska - Lincoln.

# Evaluation of the Use of Lithium Compounds in Controlling Alkali-Silica Reactivity in Concrete Pavement

Nebraska Department of Roads  
Project Number RDT-QX5(1)



**US Army Corps  
of Engineers**  
Omaha District



# **Evaluation of the Use of Lithium Compounds in Controlling Alkali-Silica Reactivity in Concrete Pavement**

**NDOR Project Number RDT-QX5(1)**

## **PRINCIPAL INVESTIGATORS**

**Christopher Y. Tuan, Ph.D., P.E.  
Associate Professor  
Department of Civil Engineering  
College of Engineering & Technology  
University of Nebraska-Lincoln**

**Michael T. Kelly, P.E.  
Civil Engineer  
US Army Corps of Engineers  
Omaha District**

**Mark E. Buss  
Geologist  
US Army Corps of Engineers  
Omaha District**

## **Sponsored by**

**Federal Highway Administration  
Nebraska Department of Roads  
and  
Center for Infrastructure Research, UNL**

**October 2005**

### Technical Report Documentation Page

1. Report No <b>RDT-QX5(1)</b>	2. Government Accession No.	3. Recipient's Catalog No.	
4. Title and Subtitle  <b>Evaluation of the Use of Lithium Compounds in Controlling Alkali-Silica Reactivity in Concrete Pavement</b>		5. Report Date <b>October 2005</b>	
		6. Performing Organization Code	
7. Author/s <b>Christopher Y. Tuan, Michael T. Kelly and Mark E. Buss</b>		8. Performing Organization Report No.	
9. Performing Organization Name and Address <b>University of Nebraska-Lincoln, and U.S. Army Corps of Engineers, Omaha District</b>		10. Work Unit No. (TRAIS)	
		11. Contract or Grant No. <b>26-1120-0008-001</b>	
12. Sponsoring Organization Name and Address <b>Federal Highway Administration, U.S. Department of Transportation, and Nebraska Department of Roads (NDOR)</b>		13. Type of Report and Period Covered  <b>Final Report</b>	
		14. Sponsoring Agency Code	
15. Supplementary Notes			
16. Abstract  Presented herein are findings from a three-year field trial in which lithium nitrate was applied on an existing concrete pavement in Norfolk, Nebraska, in the attempt to arrest on-going alkali-silica reaction (ASR) distress. Various destructive and non-destructive means were utilized to measure the effectiveness of the lithium treatments. Concrete cylinders were cored for petrographic examination and split-tension testing. Powder samples were taken to determine lithium content. Nondestructive evaluations included using crack mapping, a Schmidt hammer, a velocity ("V") meter, and an impact echo apparatus. The results to date have not shown definitive benefits of the lithium material in arresting the ASR process; however, the observed lithium penetration by gravity soaking has been very limited. Presumably the pavement has not reached the deterioration state for optimal permeability for penetration of the lithium material.  Other application techniques on hardened concrete such as surface pressurization and vacuum impregnation have been investigated to a limited extent as an alternate method to gravity soaking. The surface pressurization technique has shown promising results in so far as achieving higher lithium contents. Effort is now needed in achieving higher lithium contents on a larger scale so that a more realistic evaluation of the effects of the lithium can be preformed.			
17. Key Words <b>Alkali-silica reaction, lithium nitrate, portland cement concrete, pavement, nondestructive evaluations.</b>		18. Distribution Statement <b>No restriction. This document is available to the public through the Nebraska Department of Roads.</b>	
19. Security Classification (of this report) <b>Unclassified</b>	20. Security Classification (of this page) <b>Unclassified</b>	21. No. of Pages <b>108</b>	22. Price

**Form DOT F 1700.7 (8-72) Reproduction of form and completed page is authorized**

## **DISCLAIMER**

The contents of this report reflect the views of the authors who are responsible for the facts and the accuracy of the data presented herein. The contents do not necessarily reflect the official views or policies of the U.S. Federal Highway Administration, Nebraska Department of Roads, the University of Nebraska-Lincoln nor the U.S. Army Corps of Engineers. This report does not constitute a standard, specification, or regulation. Trade or manufacturers' names which may appear in this report are cited only because they are considered essential to the objectives of the report. Neither the United States (U.S.) government, the University of Nebraska nor the State of Nebraska endorses products or manufacturers referenced herein.

## **Acknowledgments**

The financial supports provided by the U.S. Department of Transportation, Federal Highway Administration, the Nebraska Department of Roads, and the Center for Infrastructure Research (CIR) of the University of Nebraska-Lincoln are gratefully acknowledged. The Public Works Department of the City of Norfolk, Nebraska, is also gratefully acknowledged for providing the test site along with personnel and materials during the field work for this project.

# Table of Contents

Technical Report Documentation .....	i
Disclaimer .....	ii
Acknowledgements .....	iii
Table of Contents .....	iv

## List of Tables

- ❑ Table No. 1 – Concrete Mix Design
- ❑ Table No. 2 – Splitting Tensile Strengths
- ❑ Table No. 3a – Impact Echo Data (Panel 6, Control Phase II)
- ❑ Table No. 3b – Impact Echo Data (Panel 7, Treated Phase II)
- ❑ Table No. 3c – Impact Echo Data (Panel 17, Control Phase I)
- ❑ Table No. 3d – Impact Echo Data (Panel 18, Treated Phase I)
- ❑ Table No. 4a – V-Meter Data (Panel 6, Control Phase II)
- ❑ Table No. 4b – V-Meter Data (Panel 7, Treated Phase II)
- ❑ Table No. 4c – V-Meter Data (Panel 17, Control Phase I)
- ❑ Table No. 4d – V-Meter Data (Panel 18, Treated Phase I)
- ❑ Table No. 5a – Schmidt Hammer Data (Panel 6, Control Phase II)
- ❑ Table No. 5b – Schmidt Hammer Data (Panel 7, Treated Phase II)
- ❑ Table No. 5c – Schmidt Hammer Data (Panel 17, Control Phase I)
- ❑ Table No. 5d – Schmidt Hammer Data (Panel 18, Treated Phase I)

## List of Figures

- ❑ Figure 1 – Test Panel Layout
- ❑ Figure 1a – Test Panel Layout
- ❑ Figure 2 – Saw Cut Detail
- ❑ Figure 3 – Instrumentation Plan
- ❑ Figure 4 – DeMac Point Detail

## List of Acronyms

ASR: Alkali-Silica Reaction

EDX: Energy Dispersive X-Ray Fluorescence Spectrometry

FHWA: Federal Highway Administration

K<sub>2</sub>O: Potassium Oxide

lbs: pounds

LiOH: Lithium Oxide

LiNO<sub>3</sub>: Lithium Nitrate

NDT: Non-Destructive Evaluation Techniques

Na<sub>2</sub>O: Sodium Oxide

SEM: Scanning Electron Microscopy

SHRP: Strategic Highway Research Program

SSD: Saturated Surface Dry

TOC: table of contents

USACE: United States Army Corps of Engineers

V-Meter: Velocity Meter



## **Chapter 1 - Introduction**

1.1 General .....	1
1.2 Background .....	1
1.3 Project Location & Description .....	3
1.4 Petrographic ASR Confirmation .....	4
1.5 Control and Test Panel Layout .....	5
1.6 Lithium Application Procedures .....	6

## **Chapter 2 – Field Instrumentation and Pavement Evaluation Methods**

2.1 General .....	9
2.2 Impact Echo .....	9
2.3 Schmidt Hammer .....	10
2.4 Velocity (V) Meter .....	11
2.5 Crack Mapping and Photographic Documentation .....	11
2.6 Demac Points for Strain Measurement .....	12

## **Chapter 3 - Data Evaluation**

3.1 Concrete Expansion and Contraction (Demac Points) .....	13
3.2 Crack Propagation .....	14
3.3 Concrete Quality Evaluation by Impact Echo .....	14
3.4 Concrete Quality Evaluation by Schmidt Hammer .....	15
3.5 Concrete Quality by V-Meter .....	15

## **Chapter 4 - Conclusions & Recommendations**

4.1 Conclusions .....	17
4.2 Recommendations .....	19

## **List of References**

1 - Stanton, T.E., "Expansion of Concrete Through Reaction Between Cement and Aggregate," Proceedings of ASCE, Vol.66, pp.1781-1811, 1940.

2 – Johnston, D.P., R. Surdahl and D.B. Stokes, "A Case Study of a Lithium-Based Treatment of an ASR affected Pavement," Proceedings from the 11<sup>th</sup> International Conference on Alkali Aggregate Reactions, CRIB< Quebec City, Canada, pp.1140-1158, 2000.

3 – Johnston, D.P., Mitigation of Potential Alkali-Silica Reactivity Using Lithium", SHRP Concrete and Structures ASR Showcase Test and Evaluation Project 34, 2001.

## **Photographs**

## **Appendix I - Figures**

## **Appendix II - Tables**

## **Appendix III – Data Plots**

- Exhibit No. 1 – Expansion/Contraction (Demac) Data
  - ✓ Plate No. 1: Panel No. 1 (Treated), Average East-West Movement
  - ✓ Plate No. 2: Panel No. 1 (Treated), Average North South Movement
  - Plate No. 3: Panel No. 2 (Control), Average East-West Movement
  - ✓ Plate No. 4: Panel No. 2 (Control), Average North-South Movement
  - ✓ Plate No. 5: Panel No. 11A (Treated), Average East-West Movement
  - ✓ Plate No. 6: Panel No. 11A (Treated), Average North-South Movement
  - ✓ Plate No. 7: Panel No. 14 (Control), Average East-West Movement
  - ✓ Plate No. 8: Panel No. 14 (Control), Average East-West Movement
  - ✓ Plate No. 9: East-West Expansion/Contraction, New Concrete
  - ✓ Plate No. 10: North-South Expansion/Contraction, New Concrete
  - ✓ Plate No. 11: East-West Expansion/Contraction, Old Concrete
  - ✓ Plate No. 12: North-South Expansion/Contraction, Old Concrete
  - ✓ Plate No. 13: East-West Expansion/Contraction

- ✓ Plate No. 14: North-South Expansion/Contraction
- Exhibit No. 2 – Crack Mapping
  - ✓ Plate No. 1: Panel 6, No. 2
  - ✓ Plate No. 2: Panel 6, No. 3
  - ✓ Plate No. 3: Panel 6, No. 4
  - ✓ Plate No. 4: Panel 6, No. 5
  - ✓ Plate No. 5: Panel 7, No. 1
  - ✓ Plate No. 6: Panel 7, No. 2
  - ✓ Plate No. 7: Panel 7, No. 3
  - ✓ Plate No. 8: Panel 17, No. 1
  - ✓ Plate No. 9: Panel 17, No. 2
  - ✓ Plate No. 10: Panel 17, No. 3
  - ✓ Plate No. 11: Panel 17, No. 4
  - ✓ Plate No. 12: Panel 18, No. 3
- Exhibit No. 3 – Impact Echo Data
- Exhibit No. 4 – Schmidt Hammer Data
- Exhibit No. 5 – “V” Meter Data
- Exhibit No. 6 – Lithium Content Data
  - ✓ Plate No. 1: Lithium Content by Gravity Soaking, Oct 03
  - ✓ Plate No. 2: Lithium Content by Gravity Soaking, Jun 05
  - ✓ Plate No. 3: Lithium Content, Flood Coat, Old Concrete vs. New Concrete
  - ✓ Plate No. 4: Lithium Content Panel No. 17, Control
  - ✓ Plate No. 5: Lithium Content, Panel 13, Pressure Treated
  - ✓ Plate No. 6: Lithium Content Panel No. 15-1, Vacuum Impregnation
  - ✓ Plate No. 7: Maximum Lithium Content
  - ✓ Plate No. 8: Average Lithium Content in Upper 4 “

## **Chapter 1 Introduction**

### **1.1 General**

In FY 2000, the Federal Highway Administration (FHWA) was directed by Congress to fund a program of research and implementation of lithium-based technologies for the mitigation of alkali-silica reactivity (ASR) in Portland cement concrete. Two types of field trials were considered: (1) New construction or reconstruction projects using lithium-based technologies to prevent ASR, and (2) Application of lithium-based technologies on existing hardened concrete to mitigate ASR. The objective of these field trial studies was to demonstrate the use of lithium-based technologies to state transportation agencies and to document field performance of these technologies.

Studies have shown that adding lithium compounds to concrete in the plastic state to be effective in the control of ASR. Lithium-based technology; however, has not been widely applied to existing and aged concrete bridge decks and pavements. The goals and objectives of this current project were to evaluate the ability of lithium nitrate to arrest the ASR attack in hardened concrete and to develop materials and specifications for field implementation.

### **1.2 Background**

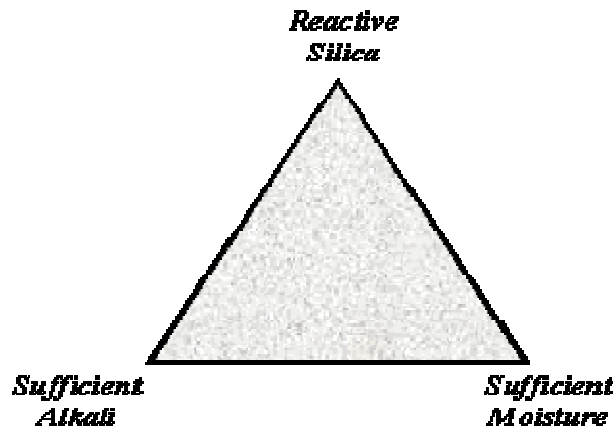
Alkali-Silica Reaction (ASR), which was first documented by Stanton<sup>[1]</sup> in 1940, is the most recognized cause of the deterioration of highway concrete structures and pavements in the United States. ASR takes place between certain reactive siliceous aggregates (e.g., opal, chalcedony and volcanic glass) and the alkali ( $\text{Na}_2\text{O}$  and  $\text{K}_2\text{O}$ )

from Portland cement paste and external sources. A reaction product gel forms that, in the presence of water, expands and may result in cracking of mortar and concrete. These surface cracks are aggravated by winter deicing salts and freeze-thaw action, leading to shallow delaminations, rebar corrosion, potholes, and other serious problems including structural failure. Three conditions are required for the reaction to take place: high alkali content (sodium and potassium) primarily from the cement, reactive silica or silicate in the aggregate and sufficient moisture in the concrete. The mechanism governing ASR and its expansion is rather complex. Several schools of thought about this phenomenon have been presented over the years. In its simplest form, ASR can be visualized as a two-step process [2]:

Step 1: Silica + Alkali + Moisture → silicate gel (ASR gel)

Step 2: ASR gel + Additional moisture → Expansion

For ASR to occur, three essential components must be present as shown in the following diagram: (1) reactive forms of silica in the aggregate, (2) sufficient alkalis primarily from the cement, and (3) sufficient moisture.



ASR Triangle

Previous studies conducted under the SHRP program [3] have shown that the addition of certain lithium-based admixtures such as lithium hydroxide (LiOH) or lithium nitrate (LiNO<sub>3</sub>), to fresh concrete will significantly reduce the ASR gel expansion. Research has also been conducted using lithium to treat hardened concrete; however, minimal documentation of “measurement” of the effects of lithium is available.

### 1.3 Project Location and Description

The structure selected for this study is a nine (9) inch thick concrete pavement located at the intersection of a 4-lane road in the North-South directions (First Street) and a two-lane road in the East-West directions (Bluff Avenue) in Norfolk, Nebraska. The pavement was constructed in two phases, Phase I and Phase II. Phase I of the pavement was constructed in 1994, while the Phase II was constructed in 1997. The mix design identifying the components of the concrete mix is presented in Table No. 1 (Appendix II) for information.

Eighteen (18) 9 feet × 9 feet panels were selected for instrumentation and evaluation as shown in Figure Nos. 1 and 1a, Appendix I. Of the eighteen (18) panels, twelve (12) panels were designated as “test panels” and six (6) panels as “control panels.” Control sections were established for base-line references to document and differentiate from the ASR-induced expansion of lithium treated and untreated portions of the pavement.

The test site was surveyed prior to the initiation of the actual instrumentation and lithium application to confirm the presence of ASR. Visible longitudinal cracks subdivided in a polygonal pattern along with a gel material were observed indicating ASR expansion-related distress as shown in Photo Nos. 1 & 2.

#### **1.4 Petrographic ASR Confirmation**

A detailed petrographic examination was performed on concrete cores obtained from the site to ascertain the presence of ASR gel product. A petrographic analysis was performed on 4-inch diameter core samples to determine the concrete condition, quality, and cause for surface cracking. The coring locations are indicated in Figure 1, Appendix I. The cored concrete samples were composed of 1-inch crushed limestone, angular to round siliceous sand, and hydrated Portland cement paste matrix. The concrete contained both entrapped and entrained air voids that appeared to be of normal distribution. The presence of entrapped air voids in the paste matrix was due to incomplete consolidation, but did not appear to be

excessive. The core surfaces were flat and relatively smooth, with several irregular shaped fractures transecting the surface. The fractures were filled with soft, carbonated alkali-silica gel precipitate. The mechanism that caused distress in the pavement appeared to be due to deleterious expansion associated with ASR attack on reactive fine aggregate particles. Numerous fine aggregate particles were surrounded by micro-cracked, darkened, reaction-rims due to gel saturation. Scanning Electron Microscopy (SEM) with Energy Dispersive X-ray Fluorescence Spectrometry (EDX) characterization of the ASR gel indicated the presence of elemental sodium and potassium, typical of an expansive ASR gel. These conditions are characteristic of concrete distress associated with ASR expansion. Other forms of concrete deterioration such as freeze-thaw, alkali-carbonate, sulfate attack, chloride attack, or excessive surface pop-out formation were not evident during the examination.

Specimens of Phase II concrete were cored from Panels No. 1 and 2, while specimens of Phase I concrete were cored from Panels No. 17 and 18. These cored cylinders were subjected to the splitting-tension tests in accordance with the ASTM C 496. Panel No. 17 was in such poor condition that the specimen broke during coring. The splitting-tensile strengths of these specimens are presented in Table No. 2 of Appendix II. As can be observed, the tensile strength of the cores taken from the treated panels was somewhat higher than taken from the untreated panels.



## **1.5 Control and Test Panel Layout**

In the effort to allow the test panels to “react” or not “react” to the ASR mechanism, each test panel was outlined with a full depth (9”) saw cut to free it from the surrounding concrete slab, as shown in Photo Nos. 3 & 4. The saw cut was then filled with compressible filler and sealed to prevent the entry of water and debris as shown in Figure No. 2, Appendix I.

In-situ non-destructive testing was conducted on the lithium-treated and untreated pavement panels. Non-destructive evaluation (NDE) techniques were used to characterize the pavement condition prior to and following lithium treatments. Those techniques included crack mapping, photographic survey, impact echo test, Velocity (V) meter test, Schmidt Hammer test, and expansion/contraction measurements.

## **1.6 Lithium Application Procedures**

Initially a liquid solution containing 30 percent lithium nitrate and a surfactant was applied to the pavement surface at the rate of 0.012 gallons per square foot (12.35 gallons per 1000 square feet). Prior to application, the concrete pavement surface was saturated with water and then allowed to drain and dry to a saturated surface dry (SSD) condition. The lithium material was measured out in a container of known volume, poured onto the test panels and distributed with the use of a broom as shown in Photo Nos. 5 & 6. It was extremely difficult to physically contain the material within the area to be treated and avoid runoff. This made it difficult to maintain the desired lithium dosage. Following evaporation of the lithium material a

gray in color, dense “lithium salt” residue appeared on the pavement surface as shown in Photo Nos. 7 & 8. The addition of water, as the evaporation process progressed, only aggravated the runoff problem. In an effort to minimize the runoff problem, the dosage was cut in half to 0.006 gallons per square feet. The pavement surface was again treated with water to achieve an SSD condition, and the lithium material applied and distributed with the use of a broom/paint roller. A similar runoff problem was encountered but to a lesser degree. The deposition of a lithium salt was again encountered upon evaporation following this procedure. In the third trial, the lithium was placed on a “dry” pavement at the rate of 0.006 gallons per square foot. The material was then distributed with the use a 9-inch long nap paint roller. As the material soaked in as well as evaporated; however, minimal “salting” was observed. Small amounts of water were sprayed on the test panels using a garden watering can as shown in Photo Nos. 9, 10 & 11 as salt appeared to promote “soaking in” of the lithium material. The salting did not reappear. In addition, runoff was minimal using this method. The lithium treatment (quantities and dates) was applied as indicated on Figure No. 1 and 1a, Appendix I.

In addition to gravity soaking of the pavement with the lithium solution, limited pressure injection and vacuum impregnation was also investigated.

In the attempt to “force” the lithium into the concrete, pressure cells, approximately 3 feet square, were constructed and anchored to the pavement surface as shown on Photo Nos. 12, 13, 14, 15 & 16. Silicone caulk was used to seal the base of the cell

to prevent loss of the lithium during pressurization. After sealing the pressure cell was filled with the lithium solution and a positive pressure applied.

In the attempt to “draw” the lithium into the concrete, a reservoir using a bead of caulk was constructed as shown in Photo No. 17. A full depth hole was drilled through the concrete pavement within the “reservoir”. A vacuum was then drawn with the use of a shop vac as shown on Photo No. 18.

## **Chapter 2 Field Instrumentation and Pavement Evaluation Methods**

### **2.1 General**

Various non-destructive evaluation (NDE) techniques were utilized to evaluate the pavement condition prior to and following the lithium treatments. These techniques included impact echo testing, Schmidt Hammer, V-meter testing, crack mapping, photographic survey, and expansion and contraction measurements. The locations of all the nondestructive tests conducted on a typical concrete panel are presented in Figure 3, Appendix I.

As discussed in Chapter 1, to relieve the compression built up in the pavement due to the ASR expansion and /or other mechanisms and to allow the treated and control panels to freely “react”, each of the 9-ft by 9-ft panels was saw-cut at the perimeter. The joints were 0.25 in. wide and through the full depth of the 9-inch pavement thickness. The joints were filled with a preformed backer rod and sealed with a flexible joint sealant afterwards.

### **2.2 Impact Echo**

The impact-echo encompasses a complete system consisting of a portable computer, test control and analysis software, a hand-held scanning unit containing six impactors and a sensitive displacement transducer as shown in Photo No. 19. A transient stress pulse is introduced into a plate-like test structure by a mechanical impact on the surface. The stress pulse consists of P and S waves, which propagate into the

structure along spherical wavefronts, and an R wave, which propagates along the surface on a circular wavefront centered at the impact point. The P and S waves are reflected by internal cracks and voids and the boundaries of the structure. The arrival of these reflected waves, which were measured by a receiving transducer, were displaced at the surface where the impact was generated. The theory states that increased displacement would suggest an increase in cracks and other voids.

### **2.3 Schmidt Hammer**

Although the Schmidt hammer does not provide a direct index of ASR distress, this instrument does provide for a relative measurement of concrete quality. A Type M Schmidt hammer as shown in Photo No. 20 was employed for quantifying the relative strength and evaluating the quality of concrete of the pavement panels. In testing, a “rebound number” is registered which is dependent upon the strength of the mortar (i.e., concrete without coarse aggregate) close to the surface. Since the strength of the mortar determines the strength of the concrete as a rule, the rebound number gives an indication of the strength of the concrete. Higher values suggest better quality and higher strength of concrete. The correlation between rebound number and strength of the concrete has been derived from a great number of hammer tests on cubes,

each cube being crushed in the machine immediately after carrying out the hammer tests. The mean error is approximately  $\pm 20$  percent for low quality concrete and  $\pm 15$  percent for high-strength concrete. The uncertainty inherent in this

correlation is slight. Three readings were taken at each location. The average of the readings was then used to determine the concrete quality at that particular point.

#### **2.4 Velocity (V) Meter**

The V-meter is composed of an ultrasonic, pulse-velocity system widely used for quality control and evaluation of concrete structures. The V-meter can assess the uniformity and relative quality of concrete, to indicate the presence of voids and cracks, to estimate the depth of cracks, and to evaluate the effectiveness of crack repairs. Poisson's ratio and modulus of elasticity of the concrete also can be calculated using S-wave transducers. Since the pulse velocity depends only on the elastic properties of the material and not on the geometry, it is a very convenient technique for evaluating concrete quality. The testing apparatus consists of a pulse generator, a pair of transducers (transmitter and receiver), an amplifier, a time measuring circuit, and a time display unit as shown in Photo No. 21. The transmitter and receiver were placed at distances of 3, 6, and 9 inches apart at each location.

#### **2.5 Crack Mapping and Photographic Documentation**

Surface cracks, spalls and other surface defects serve as indicators of concrete deterioration. Crack mapping along with photographic documentation on all the panels was conducted prior to and at various intervals following the lithium treatments. Five (5) one-foot square areas were identified for detailed crack mapping in each of the eighteen (18) panels. A 1-foot by 1-foot wood frame as shown in Photo No. 22 was fabricated for the "picture frame." A clear plastic sheet was then

placed under the frame, and cracks, holes and other apparent surface defects were then traced onto the plastic sheets. Each one of the five (5) areas was tied to specific reference point locations for future repeatability. The locations of cracking mapping locations on the concrete panels are shown in Figure 3, Appendix I.

Photographic documentation of cracks and other defects located inside the “picture frames” was also established to monitor further surface deterioration in both the treated and the untreated slabs with time.

## **2.6 Demac Points for Strain Measurement**

As a means to physically measure expansion and contraction of the concrete pavement, stainless steel knurled pins (or Demac points) having 1-mm diameter pin hole on the top, were inserted and grouted into pre-drilled holes in the pavement, as shown on Figure No. 4, Appendix I and in Photo Nos. 23 & 24. The depth of the drilled holes was such that the top of the pins were located approximately 0.25” below the pavement surface. There were nine (9) Demac points installed in each panel as previously shown in Photo No. 24. A four (4)-ft long, digital caliper with an accuracy of 0.001 inch was used to measure the distances between adjacent Demac points, as shown in Photo No. 25. All distances were read twice (i.e., in both directions) and then averaged to ensure data accuracy. Initial measurements along with ambient temperature readings were recorded before lithium treatment for a baseline reference. Following the initial measurements, the drilled holes were sealed with a flexible sealant that could be removed at a later time for subsequent

measurements. The primary purpose of the sealant was to protect the Demac points and prevent debris from entering the drilled holes.



## Chapter 3 Data Evaluation

### 3.1 Concrete Expansion and Contraction (Demac Points)

Initial distances between Demac points were measured following installation on 9 December 2002. The second set of expansion/contraction measurements was taken on 27 May 2003. Each slab was then saw-cut full depth (9-in.) parallel to the existing joints and/or exterior edges. Expansion/contraction measurements were again taken on 29 May 2003. An analysis of the data revealed that all of the panels experienced a stress relief (expansion/contraction) following the saw cut. The most recent measurements were taken on 15 June 2005. All of the panels experienced a net growth (expansion) except Panel No. 8 from the time of saw cut operation until June 2005. Panel No. 8 experienced 0.01% contraction in the east-west direction and a 0.01% expansion in the north-south directions. Typical expansion/contraction data plots for both treated and control panels are presented on Plate Nos. 1 thru 8 in Exhibit No. 1, Appendix III. A summary of the east-west expansion/contraction data for the Phase II concrete (new) is presented on Plate No. 9, Exhibit No.1, Appendix III. A summary of the north-south expansion/contraction data for the Phase II concrete (new) is presented on Plate No.10, Exhibit No.1, Appendix III. A summary of the east-west expansion/contraction data for the Phase I concrete (old) is presented on Plate No.11, Exhibit No.1, Appendix III. A summary of the north-south expansion/contraction data for the Phase I concrete (old) is presented on Plate No.12, Exhibit No.1, Appendix III. Plate Nos. 13 & 14 in Exhibit No. 4, Appendix III presents the overall east-west/north-south expansion/contraction of all of the panels.

As can be observed, the older panels (Phase I) exhibited a greater degree of expansion than did the newer (Phase II) concrete. The “treated” panels actually exhibited a greater degree of expansion than did the “control” panels. Possibly the panels experienced a pessimism effect.

### **3.2 Crack Propagation**

Crack mapping was used to document progressive deterioration of the concrete slabs. As described previously, five (5) 1-foot square areas were established in each of the 18 panels. Details of crack pattern and other surface defects of all the slabs were initially mapped in October 2002 for baseline references. Panel Nos. 6, 7, 17 and 18 were also mapped in May 2004 and June 2005. This information is presented on Plate Nos. 1 thru 12 in Exhibit No. 2, Appendix III. It is evident that there is significant crack development in the untreated panel (No.17) as compared to the treated panel (No.18). There has been only minor crack growth in the Phase II panels (Panels 6 & 7) with no appreciable difference between the control and the treated panels.

### **3.3 Concrete Quality Evaluation by Impact Echo**

The quality of panel Nos. 6, 7, 17 and 18 were evaluated by using the impact echo apparatus in October 2002, October 2003 and May 2004. Numerical impact echo data obtained in October 2002 and May 2004 is presented in Table Nos. 3a, 3b, 3c & 3d, Appendix II.

A graphical summary of the data is presented in Exhibit No. 3, Appendix III. With the exception of the October 2003 data, the October 2002 data and the May 2004 data are comparable, except for Panel No. 6 which actually exhibited an increase in quality, indicating little difference between the treated and control panels from 2002 to 2004.

### **3.4 Concrete Quality Evaluation by Schmidt Hammer**

The Schmidt hammer is a convenient but less accurate tool for concrete quality evaluations; however, the instrument does provide for a comparison of quality over time. Numerical Schmidt Hammer data obtained in October 2002 and June 2005 is presented in Table Nos. 4a, 4b, 4c & 4d, Appendix II.

The Schmidt Hammer data obtained from the testing (Oct 02, Oct 03, May 04 & Jun 05) is presented graphically in Exhibit No. 4, Appendix III. As can be observed little change in concrete quality was exhibited between October 2002 and June 2005 using the Schmidt Hammer.

### **3.5 Concrete Quality Evaluation by V-meter**

V-Meter data was obtained from specific test panels in Oct 02, Oct 03, May 04 and Jun 05. Numerical V-Meter data obtained in October 2002 and June 2005 is presented in Table Nos. 5a, 5b, 5c & 5d, Appendix II.

V-Meter data obtained from the testing (Oct 02, Oct 03, May 04 & Jun 05) is presented graphically in Exhibit No. 5, Appendix III. Similar to the Schmidt hammer data, little change in the concrete quality was exhibited between October 2002 and May 2004; however a definite trend is apparent following the June 2005 readings. A definite decrease in concrete quality is apparent following the June 2005 reading indicating that all of the concrete, treated and untreated deteriorated at approximately the same rate.

## **Chapter 4 - Conclusions and Recommendations**

### **4.1 Conclusions**

Based on the NDT techniques utilized to evaluate the on-going ASR deterioration in both the treated and control panels, it is evident that the results to date have not shown definitive benefits of the lithium material in arresting the ASR process. The observed lithium penetration by gravity soaking; however, has been very limited. Presumably the pavement has not reached the deterioration state for optimal permeability for penetration of the lithium material.

Powder samples were obtained from the pavement, as shown on Photo Nos. 26, 27 & 28, for laboratory analysis to determine the actual lithium content. Samples were obtained from both the treated panels and the control panels for comparison. Lithium content profiles, obtained both early and late in the research, of both a treated panel (Panel 18) and a control panel (Panel 1) are presented on Plate Nos. 1 & 2, Exhibit No. 6 Appendix III. Plate No. 3, Exhibit No. 6, Appendix III presents a comparison of the average lithium content observed in the upper 4" in both the older concrete (Phase I) and the newer concrete (Phase II) when using a flood coat application method. The maximum lithium content observed in the flood coated panels was 46 PPM in Panel No. 18. Panel No. 18 is in the old Phase I concrete and has deteriorated to the point of excessive cracking and resulting high permeability. The normal "noise" level of lithium that can be expected during the testing is in the range

of 5-10 PPM which is consistent with the lithium contents determined for Panel Nos. 1, 3, & 8. The maximum lithium content in the control panel (Panel 17, Phase I) was approximately 27 PPM as shown on Plate No. 4, Exhibit No. 6, Appendix III.

It is evident that even if the lithium is beneficial in arresting ASR, adequate amounts were not achieved by the gravity flood coating method utilized in the test program to realize this benefit.

In addition to gravity soaking of the pavement with the lithium solution, limited pressure injection and vacuum impregnation was also investigated as discussed in Chapter One.

In the attempt to “force” the lithium into the concrete a pressure cell, approximately 3 feet square, was constructed and anchored to the pavement surface as shown on Photo Nos. 12, 13, 14, 15 & 16. Silicone caulk was used to prevent loss of the lithium during pressurization. The pressure cell was filled with the lithium solution with a positive pressure applied. Plate No. 5, Exhibit No. 6, Appendix III presents a lithium content profile of a treated panel using external positive pressure. Lithium contents as high as 275 PPM (Panel No. 13) were realized using a positive pressure cell.

In the attempt to “draw” the lithium into the concrete, a reservoir using a bead of caulk was constructed as shown in Photo No. 17. A full depth hole was drilled

through the concrete pavement within the “reservoir”. A vacuum was then drawn with the use of a shop vac as shown on Photo No. 18. Lithium contents as high as 102 PPM (Panel No. 15) were realized using a vacuum impregnation method. Plate No. 6, Exhibit No. 6, Appendix III presents a lithium content profile of an area in Panel No. 15 using vacuum impregnation.

Overall summaries of lithium contents using various application methods are presented on Plate Nos. 7 & 8, Exhibit No. 6, Appendix III. As can be observed, greater lithium contents were achieved using the vacuum impregnation method as compared to simply a flood coat application. The pressure injection method achieved even a higher content.

Based on the lack of benefit observed towards controlling the ASR mechanism and the limited lithium contents achieved in the flood coated panels it is concluded that the potential benefit or lack thereof of the lithium is still unknown.

#### **4.2 Recommendations**

Based on the lithium contents achieved in the limited testing using pressure injection and vacuum impregnation methods, it is concluded that achieving higher lithium contents in the hardened concrete is possible. It is recommended that cost effective means be investigated to increase the lithium content in the hardened concrete at which time the exact benefit of the lithium or lack thereof can be fully ascertained.

# **PHOTOGRAPHS**





**Photo No. 1 - ASR Damage**



**Photo No. 2 - ASR Damage**





**Photo No. 3 - Saw Cutting Operation**



**Photo No. 4 - Finished Saw Cut**



**Photo No 5 - Lithium Application**



**Photo No. 6 - Lithium Application**





**Photo No. 7 - Lithium Salt Residue**



**Photo No. 8 – Lithium Salt Residue**



**Photo No. 9 – Application of Water**



**Photo No. 10 – Application of Water.**





**Photo No. 11 - Lithium Treated Pavement**



**Photo No. 12 – Pressure Cell**

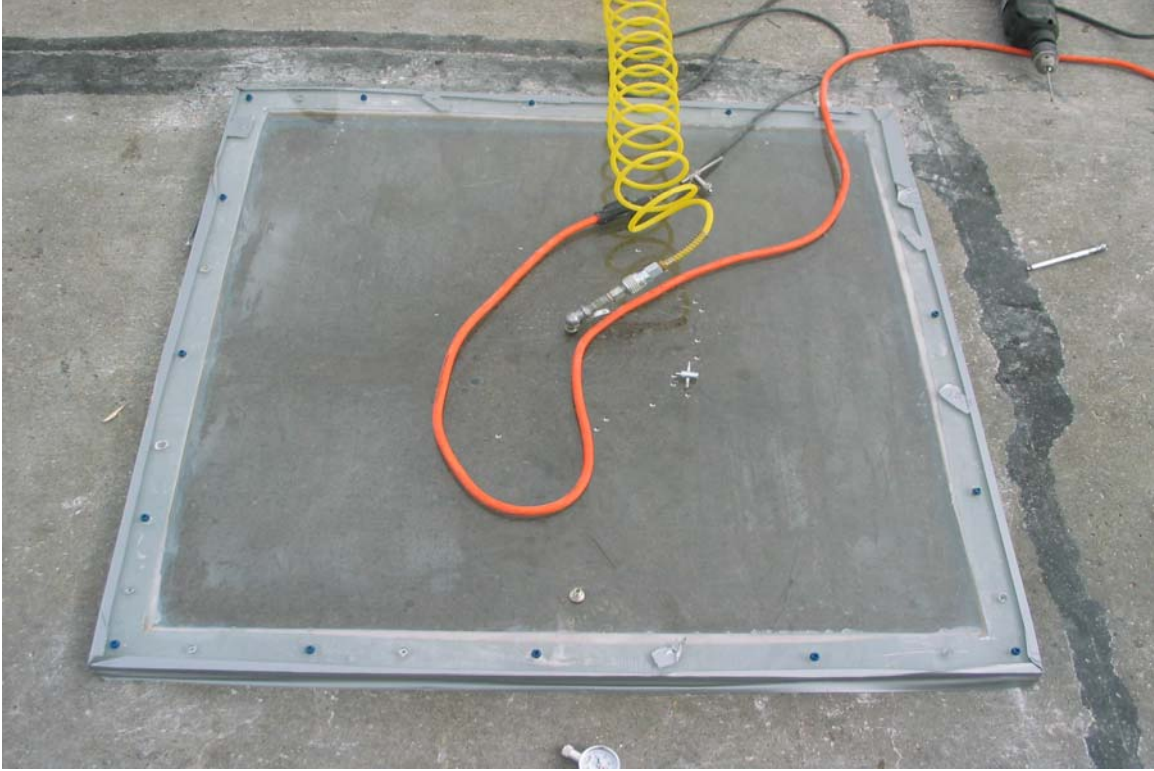


**Photo No. 13 - Pressure Cell**



**Photo No. 14 – Pressure Cell**





**Photo No. 15 - Pressure Cell**



**Photo No. 16 – Pressure Cell**





**Photo No. 17 - Vacuum Impregnation of Lithium Nitrate**

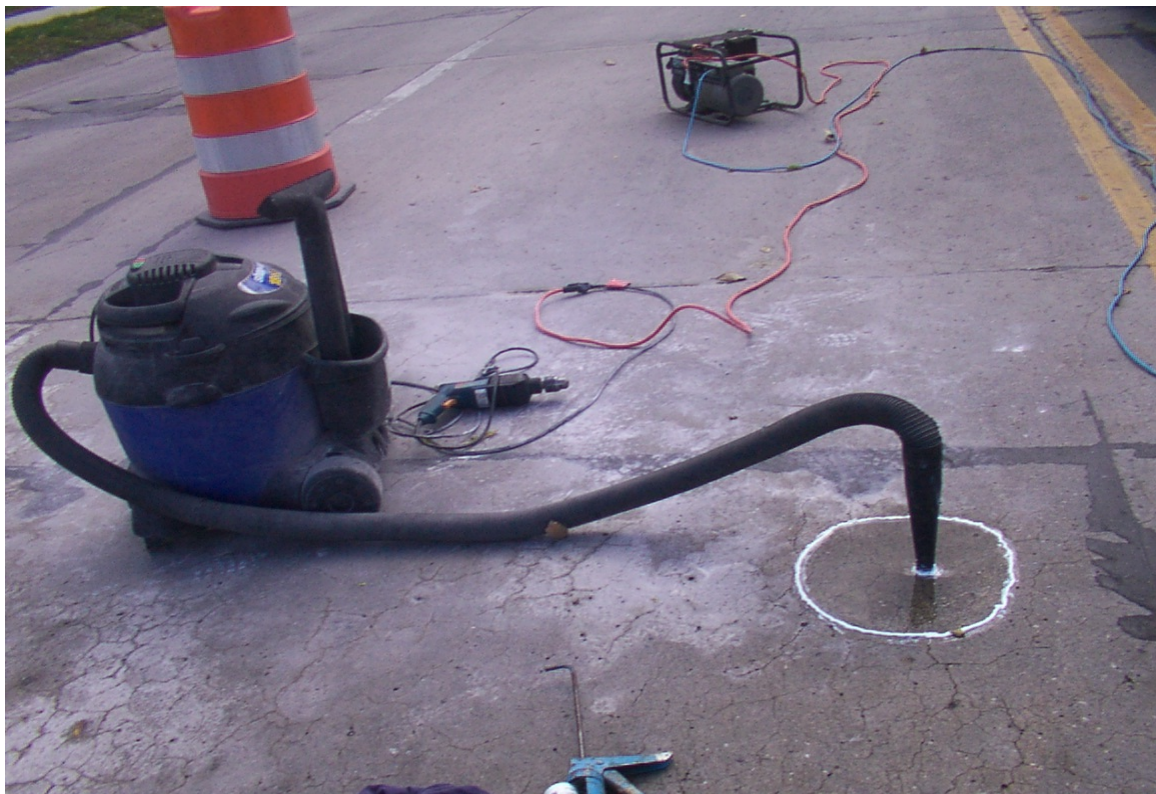


**Photo No. 18 - Vacuum Impregnation of Lithium Nitrate**



**Photo No. 19 - Impact Echo Evaluation**



**Photo No. 20 – Schmidt Hammer Evaluation**



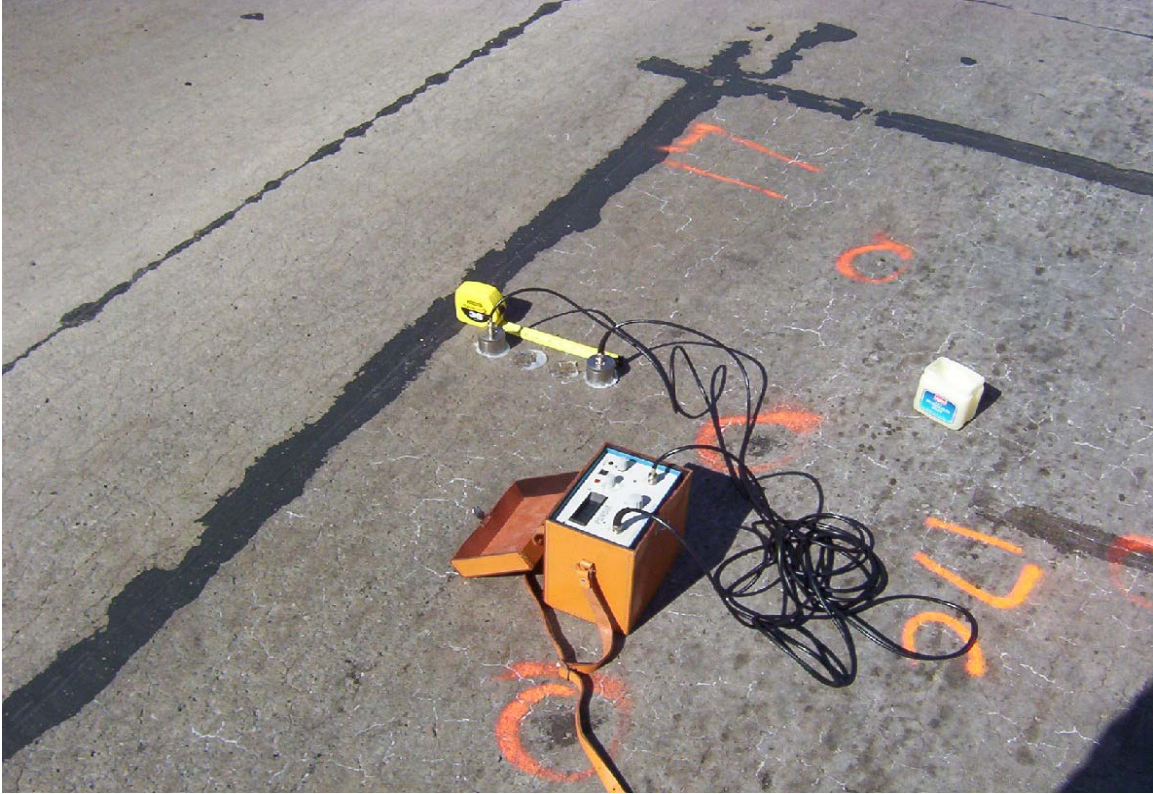


Photo No. 21 – “V” Meter Evaluation



Photo No. 22 – Crack Mapping



**Photo No. 23** – Demac Point



**Photo No. 25** – Demac Point Locations





**Photo No. 25 - Expansion / Contraction Measurements**

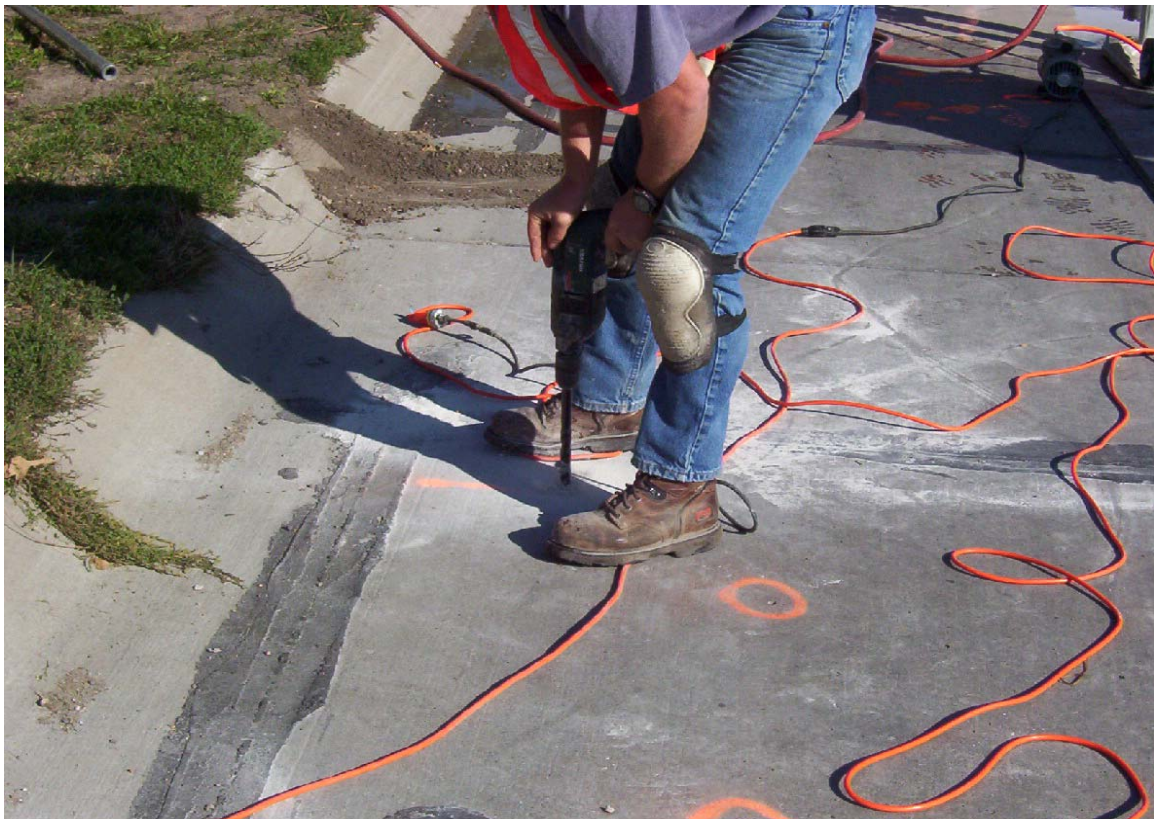


**Photo No. 26 – Powder Samples for Lithium Content**





**Photo No. 27 - Powder Samples for Lithium Content**

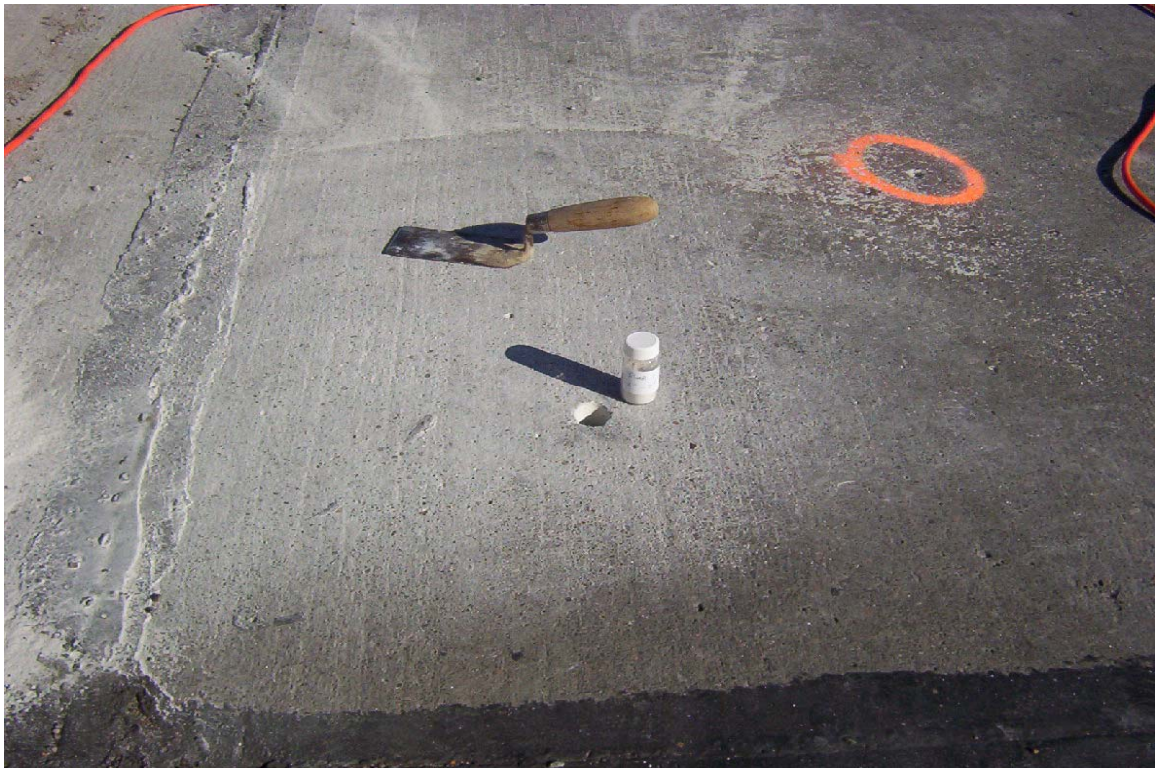
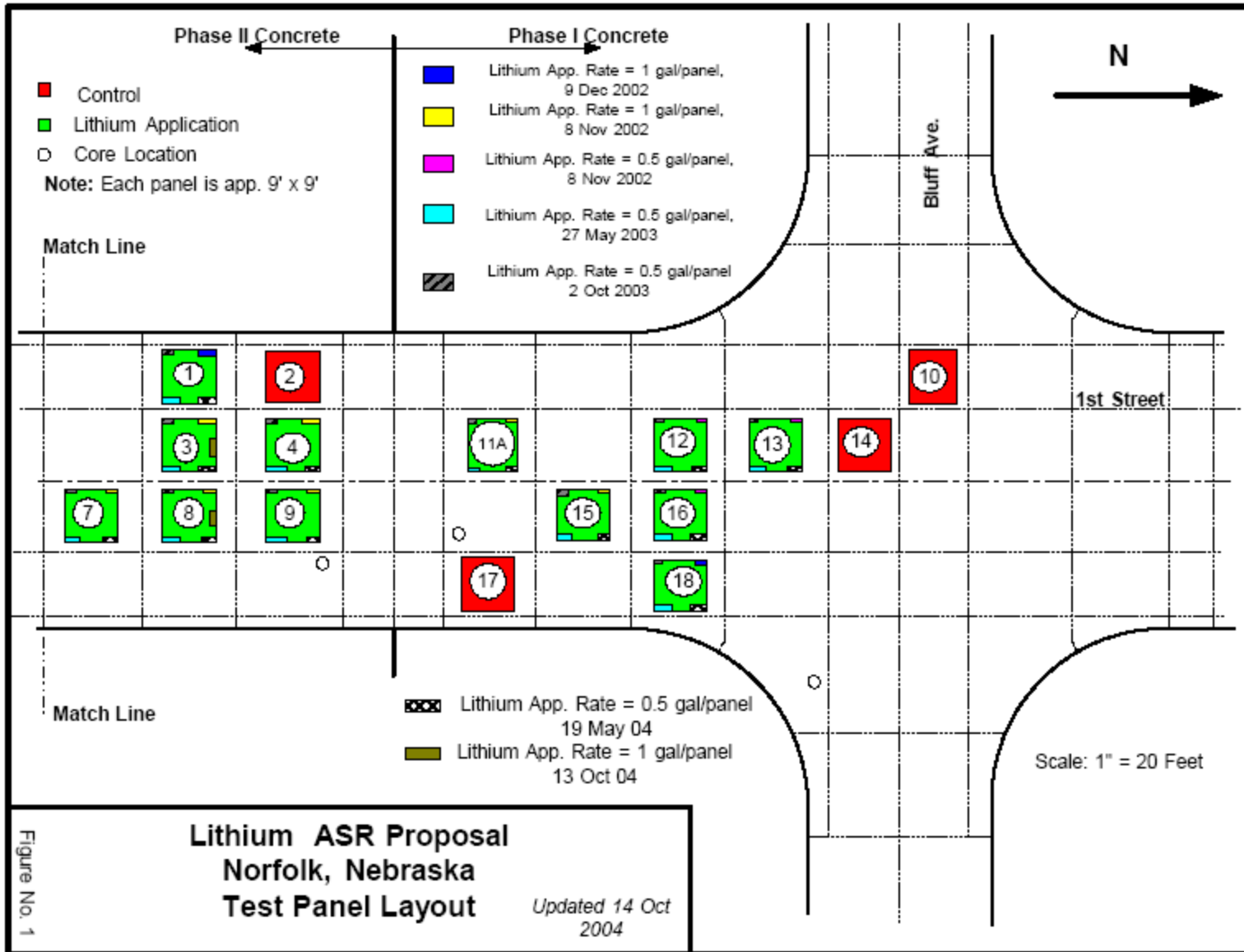


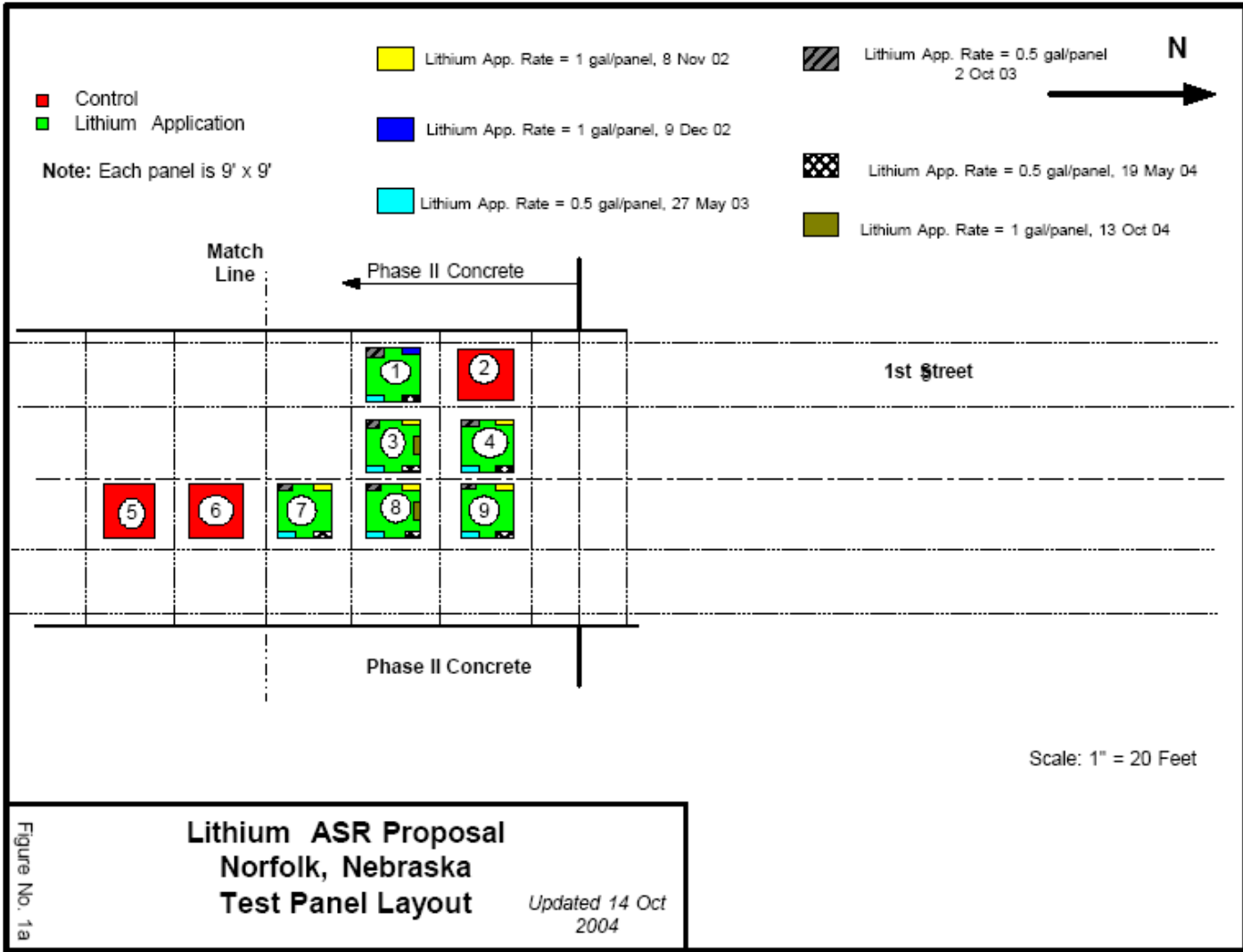
**Photo No. 28 – Powder Samples for Lithium Content**

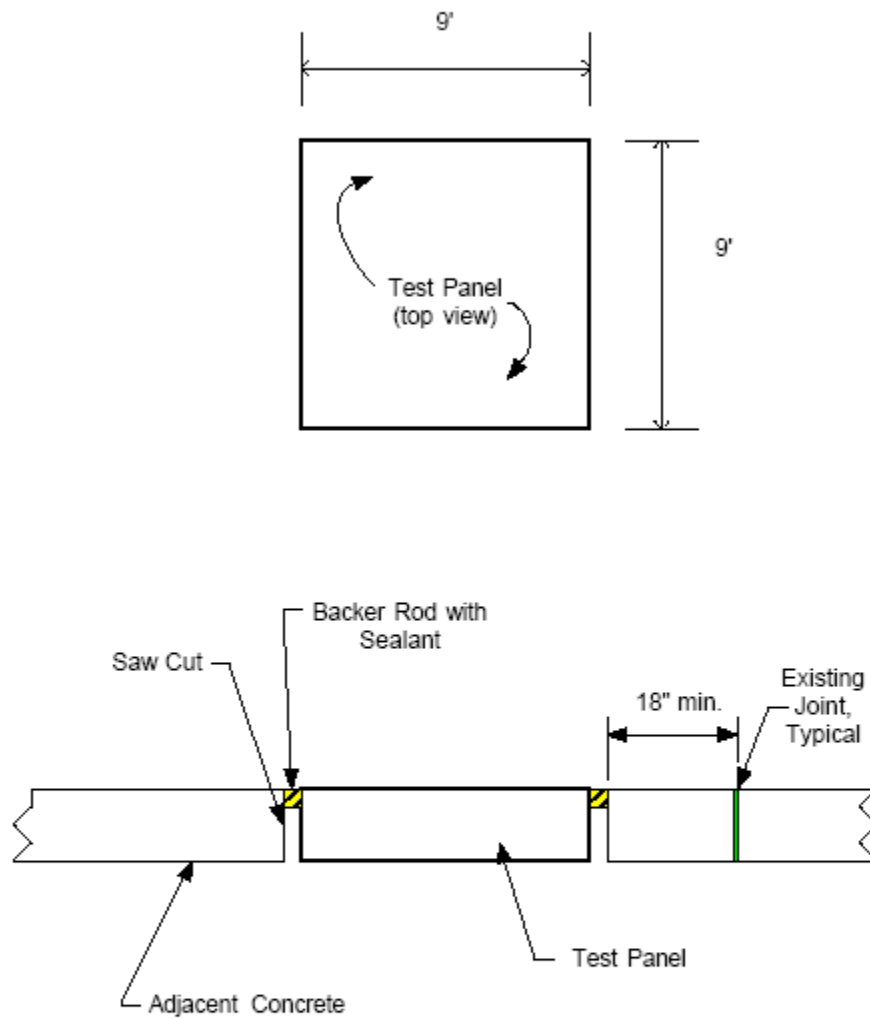
# **APPENDIX I**

# FIGURES









**Notes:**

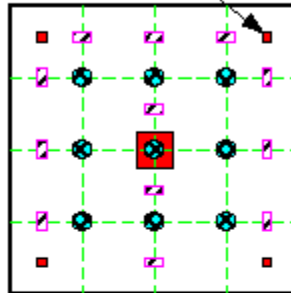
- 1.) All saw cuts were full depth.
- 2.) Panel size: 9' x 9'.
- 3.) Test point locations to be determined in the field.
- 4.) Saw cuts placed 1' from existing joints.

**Saw Cut Detail**

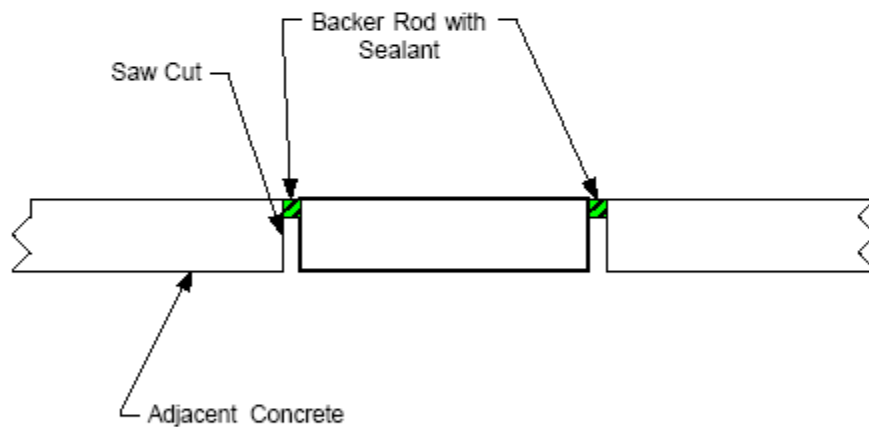
No Scale

Figure No. 2

Typical Test Points



- Map Cracking & Photographic Documentation
- - - Impact Echo
- ▨ Schmidt Hammer & V-Meter
- ⊗ Demac Points



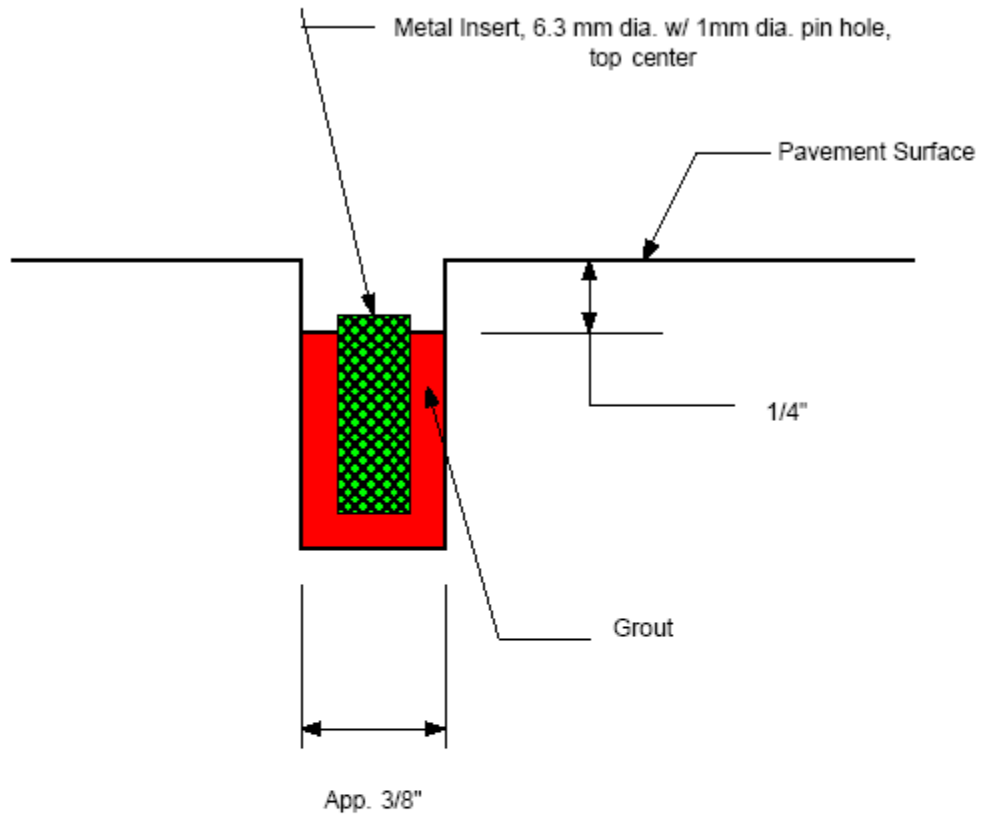
**Notes:**

- 1.) All saw cuts shall be full depth.
- 2.) Panel size: 9' x 9'.
- 3.) Test point locations to be determined in the field.

**Instrumentation Plan**

No Scale

Figure No. 3



**Pavement Insert (DeMac Point) Detail**  
(no scale)

Figure No. 4

# **APPENDIX II**

# **TABLES**

<b>Table No. 1 – Concrete Mix Design</b>	
<b>Material</b>	<b>Quantity</b>
Type I Portland Cement	564 Lbs.
Class C Fly Ash	100 Lbs.
47B Sand & Gravel*	2050 Lbs.
Water Reducer	900 Lbs.
47B Limestone	12 oz.
Air Entrainment	2 oz.
Water	24 gal.

<b>Table No. 2 - Splitting Tensile Strengths</b>				
<b>Panel No.</b>	<b>Dia. (in.) x Length (in.)</b>	<b>Ultimate Load (Lbs.)</b>	<b>Tensile Strength (PSI)</b>	<b>Treated/Untreated</b>
1	4.03 x 9.42	50,300	844	Treated
2	4.00 x 9.14	44,900	782	Untreated
17	4.00 x 4.58	9,320	324	Untreated
18	4.00 x 10.36	43,400	665	Treated

Date Tested: 27 Feb. 2004

<b>Table No. 3a – Impact Echo Data (Panel 6, Control Phase II)</b>					
<b>October 2002</b>			<b>May 2004</b>		
<b>Point</b>	<b>Wave Speed (m/s)</b>	<b>Modulus (GPa)</b>	<b>Point</b>	<b>Wave Speed (m/s)</b>	<b>Modulus (GPa)</b>
1	2240	11.6	1	3120	22.5
2	2470	14.1	2	3350	26
3	2290	12.2	3	3300	25.3
4	2290	12.2	4	3120	22.5
5	2470	14.1	5	2890	19.3
6	2060	9.8	6	3350	26
7	2240	11.6	7	3390	26.6
8	2240	11.6	8	3350	26
9	2240	11.6	9	3390	26.6
10	2020	9.5	10	3350	26
11	2020	9.5	11	3210	23.8
12	2020	9.5	12	3530	28.9
13	2060	9.8	13	3120	22.5
14	2200	11.2	14	3440	27.4
15	1830	7.8	15	3530	28.9
16	1830	7.8	16	3440	27.4
17	2200	11.2	17	3350	26
18	2020	9.5	18	3300	25.2
19	2020	9.5	19	3440	27.4
20	2290	12.2	20	3350	26
21	-----	-----	21	3120	22.5
22	-----	-----	22	3570	29.5
23	2020	9.5	23	3390	26.6
24	2290	12.2	24	3350	26
25	1970	9.0	25	3250	24.5
<b>Average</b>		<b>10.74</b>	<b>Average</b>		<b>25.5</b>



**Table No. 3b – Impact Echo Data (Panel 7, Treated Phase II)**

October 2002			May 2004		
Point	Wave Speed (m/s)	Modulus (GPa)	Point	Wave Speed (m/s)	Modulus (GPa)
1	3340	25.9	1	3160	23.2
2	3340	25.9	2	3120	22.5
3	3110	22.4	3	2930	19.9
4	2890	19.4	4	3800	33.4
5	-----	-----	5	2890	19.4
6	2890	19.4	6	3250	24.5
7	3110	22.4	7	3350	26
8	3110	22.4	8	3300	25.2
9	3160	23.1	9	3480	28.1
10	2520	14.7	10	3530	28.9
11	3160	23.1	11	3350	26
12	3160	23.1	12	3390	26.6
13	-----	-----	13	3300	25.2
14	2930	19.9	14	3350	26
15	3070	21.8	15	3440	27.4
16	2980	20.6	16	3350	26
17	2890	19.4	17	3250	24.5
18	3070	21.8	18	3160	23.2
19	3110	22.4	19	3300	25.2
20	3110	22.4	20	3530	28.9
21	3070	21.8	21	2930	19.9
22	3110	22.4	22	3020	21.2
23	-----	-----	23	2890	19.4
24	-----	-----	24	3160	23.2
25	2840	18.7	25	2930	19.9
<b>Average</b>		<b>26.6</b>	<b>Average</b>		<b>24.5</b>

**Table No. 3c – Impact Echo Data (Panel 17, Control Phase I)**

October 2002			May 2004		
Point	Wave Speed (m/s)	Modulus (GPa)	Point	Wave Speed (m/s)	Modulus (GPa)
1	3620	30.4	1	3530	28.9
2	3340	25.9	2	2890	19.4
3	3570	29.5	3	3440	27.4
4	2840	18.7	4	2930	19.9
5	2430	13.7	5	3530	28.9
6	1790	7.4	6	2930	19.9
7	2560	15.2	7	3530	28.9
8	3440	27.4	8	3300	25.2
9	3340	25.9	9	3390	26.6
10	-----	-----	10	3480	28.1
11	3570	29.5	11	-----	-----
12	3110	22.4	12	3710	31.9
13	3570	29.5	13	3760	32.8
14	-----	-----	14	3390	26.6
15	2020	9.5	15	3300	25.3
16	2240	11.6	16	3620	30.4
17	-----	-----	17	3760	32.8
18	3110	22.4	18	3300	25.3
19	3570	29.5	19	3530	28.9
20	3570	29.5	20	3210	23.9
21	-----	-----	21	3350	26
22	3570	29.5	22	3620	30.4
23	3800	33.5	23	3760	32.8
24	2700	16.9	24	3570	29.5
25	2700	16.9	25	3480	28.1
<b>Average</b>		<b>22.6</b>	<b>Average</b>		<b>27.4</b>

**Table No. 3d – Impact Echo Data (Panel 18, Treated, Phase I)**

October 2002			May 2004		
Point	Wave Speed (m/s)	Modulus (GPa)	Point	Wave Speed (m/s)	Modulus (GPa)
1	3570	29.5	1	2890	19.4
2	3300	25.2	2	2930	19.9
3	3020	21.1	3	3350	26
4	2700	16.9	4	3020	21.2
5	2890	19.4	5	3120	22.5
6	2890	19.4	6	3160	23.2
7	2610	15.8	7	3350	26
8	3340	25.9	8	3390	26.6
9	3340	25.9	9	3160	23.2
10	3530	28.9	10	3120	22.5
11	3390	26.6	11	3390	26.6
12	3300	25.2	12	-----	-----
13	3340	25.9	13	3480	28.1
14	2890	19.4	14	3160	23.2
15	2890	19.4	15	3530	28.9
16	2930	19.9	16	2980	20.6
17	2890	19.4	17	3160	23.2
18	3070	21.8	18	3250	24.5
19	3390	26.6	19	-----	-----
20	3340	25.9	20	2890	19.4
21	2890	19.4	21	2890	19.4
22	3300	25.2	22	3300	25.2
23	2890	19.4	23	3300	25.2
24	2840	18.7	24	3300	25.2
25	2700	16.9	25	3020	21.2
<b>Average</b>		<b>22.3</b>	<b>Average</b>		<b>23.5</b>

<b>Table No. 4a – V-Meter Data (Panel 6, Control Phase II)</b>							
<b>October 2002</b>				<b>June 2005</b>			
<b>Point</b>	<b>Time (micro-sec)</b>	<b>Wave Speed (m/s)</b>	<b>Modulus (GPa)</b>	<b>Point</b>	<b>Time (micro-sec)</b>	<b>Wave Speed (m/s)</b>	<b>Modulus (GPa)</b>
1	14.2			1	12.9		
		4510	47.2			3760	32.8
2	31.1			2	33.2		
		3930	35.8			4650	50.1
3	50.5			3	49.6		
4	12.3			4	13.6		
		4080	38.6			3610	30.2
5	31			5	34.7		
		4280	42.5			4510	47.1
6	48.8			6	51.6		
7	13.8			7	13.9		
		4770	52.7			3670	31.2
8	29.8			8	34.7		
		3890	35.1			3830	34
9	49.4			9	54.6		
<b>Average</b>			<b>42</b>	<b>Average</b>			<b>37.6</b>

<b>Table No. 4b – V-Meter Data (Panel 7, Treated Phase II)</b>							
<b>October 2002</b>				<b>June 2005</b>			
<b>Point</b>	<b>Time (micro-sec)</b>	<b>Wave Speed (m/s)</b>	<b>Modulus (GPa)</b>	<b>Point</b>	<b>Time (micro-sec)</b>	<b>Wave Speed (m/s)</b>	<b>Modulus (GPa)</b>
1	13.4			1	13.8		
		4980	57.5			4280	42.5
2	28.7			2	31.6		
		4080	38.6			4190	40.7
3	47.4			3	49.8		
4	12.5			4	15.6		
		3830	35.8			3700	31.7
5	31.9			5	36.2		
		4140	39.7			4280	42.5
6	50.3			6	54		
7	14.6			7	16.3		
		4380	44.5			3910	35.4
8	32			8	35.8		
		4590	48.8			4280	42.5
9	48.6			9	53.6		
<b>Average</b>			<b>44.1</b>	<b>Average</b>			<b>39.2</b>

Table No. 4c – V-Meter Data (Panel 17, Control Phase I)							
October 2002				June 2005			
Point	Time (micro-sec)	Wave Speed (m/s)	Modulus (GPa)	Point	Time (micro-sec)	Wave Speed (m/s)	Modulus (GPa)
1	13.9			1	24.7		
		3100	22.3			1630	6.2
2	38.5			2	71.5		
		2920	19.8			1810	7.6
3	64.6			3	113.6		
4	12.9			4	23.6		
		2980	20.6			2590	15.5
5	38.5			5	53		
		2510	14.6			3510	28.6
6	68.9			6	74.7		
7	18.9			7	12.1		
		3810	33.7			2220	11.4
8	38.9			8	46.5		
		3370	26.3			3190	23.6
9	61.5			9	70.4		
<b>Average</b>			<b>22.9</b>	<b>Average</b>			<b>15.5</b>

Table No. 4d – V-Meter Data (Panel 18, Treated, Phase I)							
October 2002				June 2005			
Point	Time (micro-sec)	Wave Speed (m/s)	Modulus (GPa)	Point	Time (micro-sec)	Wave Speed (m/s)	Modulus (GPa)
1	14.5			1	17.4		
		4140	39.7			3180	23.4
2	32.9			2	41.4		
		3890	35.1			2670	16.5
3	52.5			3	70		
4	11.4			4	13.5		
		4190	40.7			3140	22.9
5	29.6			5	37.8		
		3200	23.7			3810	33.6
6	53.4			6	57.8		
7	14.6			7	18		
		3850	34.4			3470	27.9
8	34.4			8	40		
		3790	33.3			2890	19.4
9	54.5			9	66.4		
<b>Average</b>			<b>34.5</b>	<b>Average</b>			<b>24</b>

<b>Table 5a – Schmidt Hammer Data (Panel 6, Control Phase II)</b>							
<b>October 2002</b>				<b>June 2005</b>			
<b>Point</b>	<b>Ave Rebound #</b>	<b>Wave Speed (m/s)</b>	<b>Modulus (GPa)</b>	<b>Point</b>	<b>Ave Rebound #</b>	<b>Wave Speed (m/s)</b>	<b>Modulus (GPa)</b>
1	45	4070	38.3	1	46	4070	38.3
2	45	4070	38.3	2	51	3940	36
3	44	4010	37.3	3	42	4070	38.3
4	45	4070	38.3	4	45	3720	32
5	46	4120	39.3	5	45	3770	32.9
6	44	4010	37.3	6	42	3940	36
7	43	3870	36.5	7	39	3440	27.4
8	42	3940	36	8	41	3780	33.2
9	45	4070	38.3	9	46	3770	32.9
10	44	4010	37.3	10	42	3940	36
11	41	3890	35.2	11	39	3610	30.1
12	47	4160	40	12	48	3080	22
13	45	4070	38.3	13	51	3770	32.9
14	46	4120	39.3	14	49	3140	22.8
15	47	4160	40	15	46	3250	24.5
16	45	4070	38.3	16	46	3620	30.5
<b>Average</b>	<b>44.6</b>		<b>38</b>	<b>Average</b>	<b>46</b>		<b>31.6</b>

<b>Table 5b – Schmidt Hammer Data (Panel 7, Treated Phase II)</b>							
<b>October 2002</b>				<b>June 2005</b>			
<b>Point</b>	<b>Ave Rebound #</b>	<b>Wave Speed (m/s)</b>	<b>Modulus (GPa)</b>	<b>Point</b>	<b>Ave Rebound #</b>	<b>Wave Speed (m/s)</b>	<b>Modulus (GPa)</b>
1	47	4160	40	1	48	4070	37.9
2	43	3970	36.5	2	45	3940	36
3	42	3940	36	3	46	4070	37.9
4	45	4070	38.3	4	45	3720	32
5	44	4010	37.3	5	43	3770	32.9
6	44	4010	37.3	6	40	3940	36
7	44	4010	37.3	7	41	3440	27.4
8	43	3970	36.5	8	39	3780	33.2
9	43	3970	36.5	9	41	3770	32.9
10	44	4010	37.3	10	40	3940	36
11	43	3970	36.5	11	45	3610	30.1
12	43	3970	36.5	12	48	3080	22
13	45	4070	38.3	13	44	3770	32.9
14	46	4120	39.3	14	44	3140	22.8
15	45	4070	38.3	15	46	3250	24.5
16	44	4010	37.3	16	44	3620	30.5
<b>Average</b>	<b>44</b>		<b>37.4</b>	<b>Average</b>	<b>46</b>		<b>31.6</b>

<b>Table 5c – Schmidt Hammer Data (Panel 17, Control Phase I)</b>							
<b>October 2002</b>				<b>June 2005</b>			
<b>Point</b>	<b>Ave Rebound #</b>	<b>Wave Speed (m/s)</b>	<b>Modulus (GPa)</b>	<b>Point</b>	<b>Ave Rebound #</b>	<b>Wave Speed (m/s)</b>	<b>Modulus (GPa)</b>
1	39	3780	33.2	1	45	4070	38.3
2	39	3780	33.2	2	42	3940	36
3	36	3640	30.8	3	45	4070	38.3
4	37	3720	32	4	37	3720	32
5	37	3720	32	5	38	3770	32.9
6	36	3640	30.8	6	42	3940	36
7	35	3620	30.4	7	31	3440	27.4
8	36	3640	30.8	8	39	3780	33.2
9	36	3640	30.8	9	38	3770	32.9
10	37	3720	32	10	42	3940	36
11	36	3640	30.8	11	34	3610	30.1
12	34	3610	30.1	12	24	3080	22
13	36	3640	30.8	13	38	3770	32.9
14	34	3610	30.1	14	25	3140	22.8
15	25	3140	22.8	15	27	3250	24.5
16	34	3530	28.8	16	35	3620	30.5
<b>Average</b>	<b>35.4</b>		<b>30.6</b>	<b>Average</b>	<b>36</b>		<b>31.6</b>

<b>Table 5d – Schmidt Hammer Data (Panel 18, Treated, Phase I)</b>							
<b>October 2002</b>				<b>June 2005</b>			
<b>Point</b>	<b>Ave Rebound #</b>	<b>Modulus (GPa)</b>	<b>Wave Speed (m/s)</b>	<b>Point</b>	<b>Ave Rebound #</b>	<b>Modulus (GPa)</b>	<b>Wave Speed (m/s)</b>
1	44	4010	37.3	1	41	3890	35.2
2	42	3940	36	2	43	3970	36.5
3	42	3940	36	3	37	3720	32
4	39	3780	33.2	4	43	3970	36.5
5	43	3970	36.5	5	43	3970	36.5
6	43	3970	36.5	6	43	3970	36.5
7	39	3780	33.2	7	43	3970	36.5
8	48	4210	41	8	40	3850	34.3
9	44	4010	37.3	9	44	4010	37.3
10	42	3940	36	10	44	4010	37.3
11	49	4240	41.7	11	44	4010	37.3
12	47	4160	40	12	43	3970	36.5
13	45	4070	38.3	13	44	4010	37.3
14	45	4070	38.3	14	44	4010	37.3
15	44	4010	37.3	15	42	3940	36
16	44	4010	37.3	16	40	3850	34.3
<b>Average</b>	<b>43.8</b>		<b>37.2</b>	<b>Average</b>	<b>44</b>		<b>36.1</b>

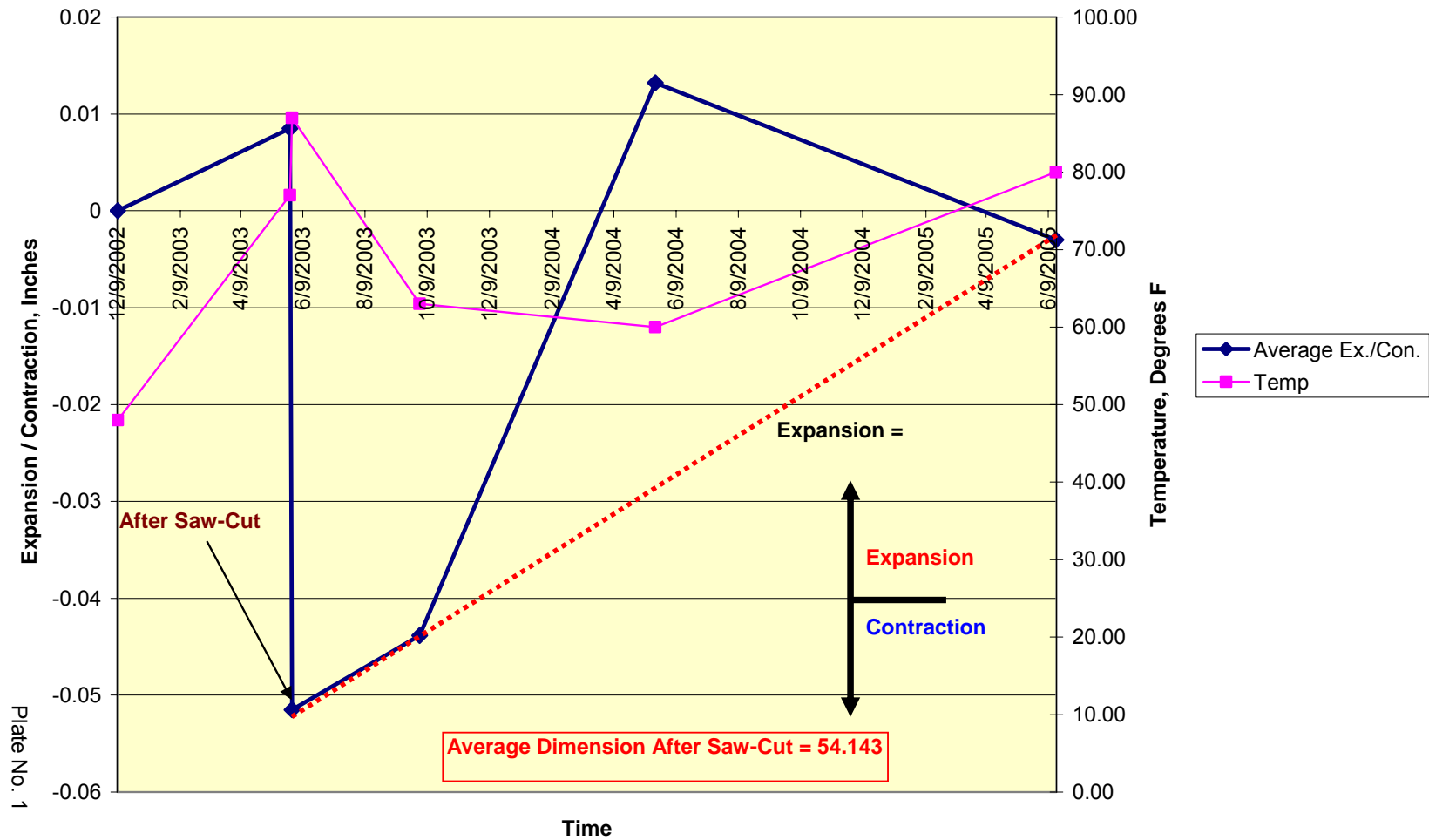
# **APPENDIX III**



# DATA PLOTS

# **EXHIBIT NO. 1**

**Panel No. 1 (Treated)**  
**Average East-West Movement**



Panel No. 1 (Treated)  
Average North - South Movement

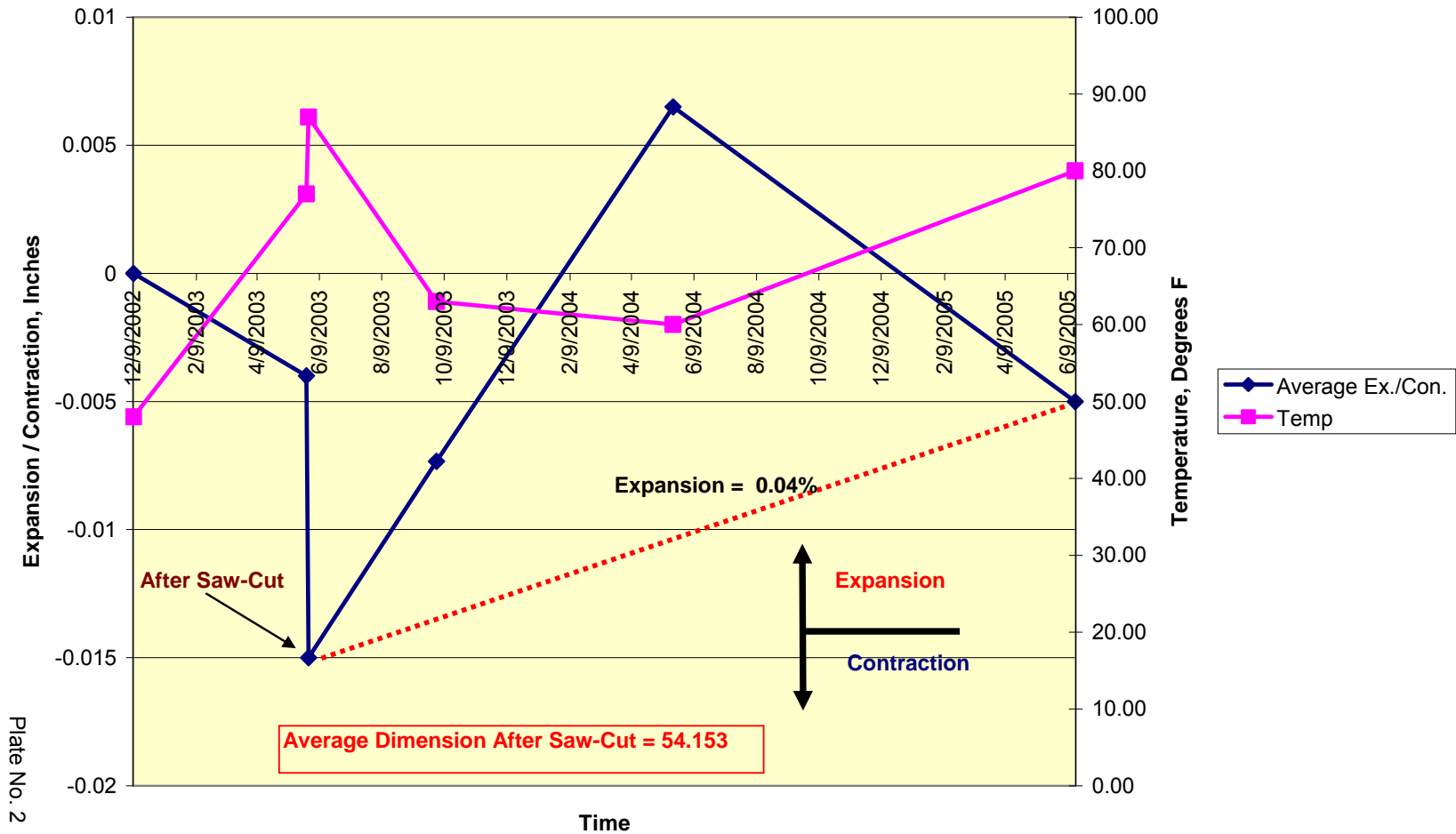
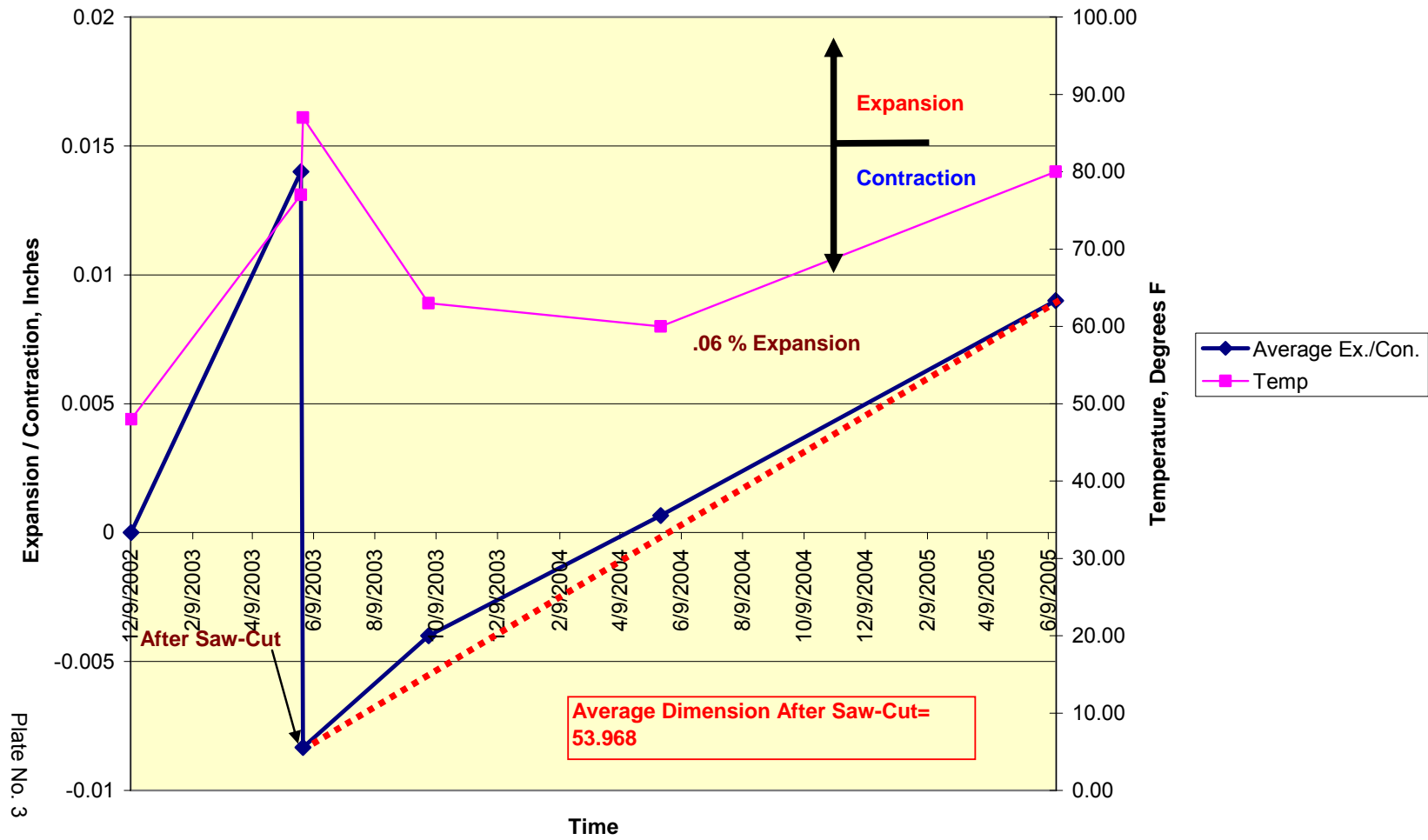


Plate No. 2

**Panel No. 2 (Control)**  
**Average East-West Movement**



**Panel No. 2 (Control)**  
**Average North - South Movement**

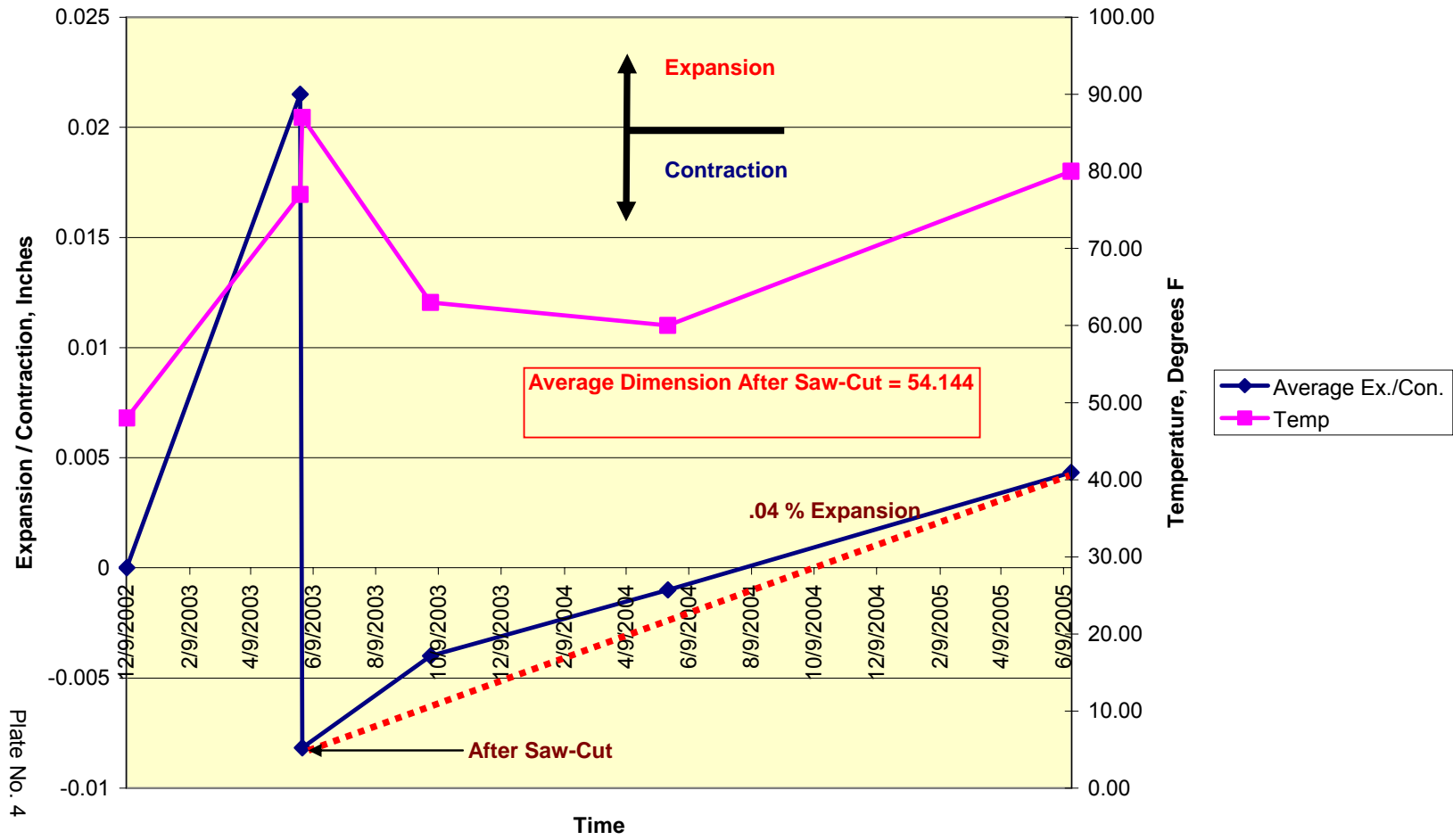
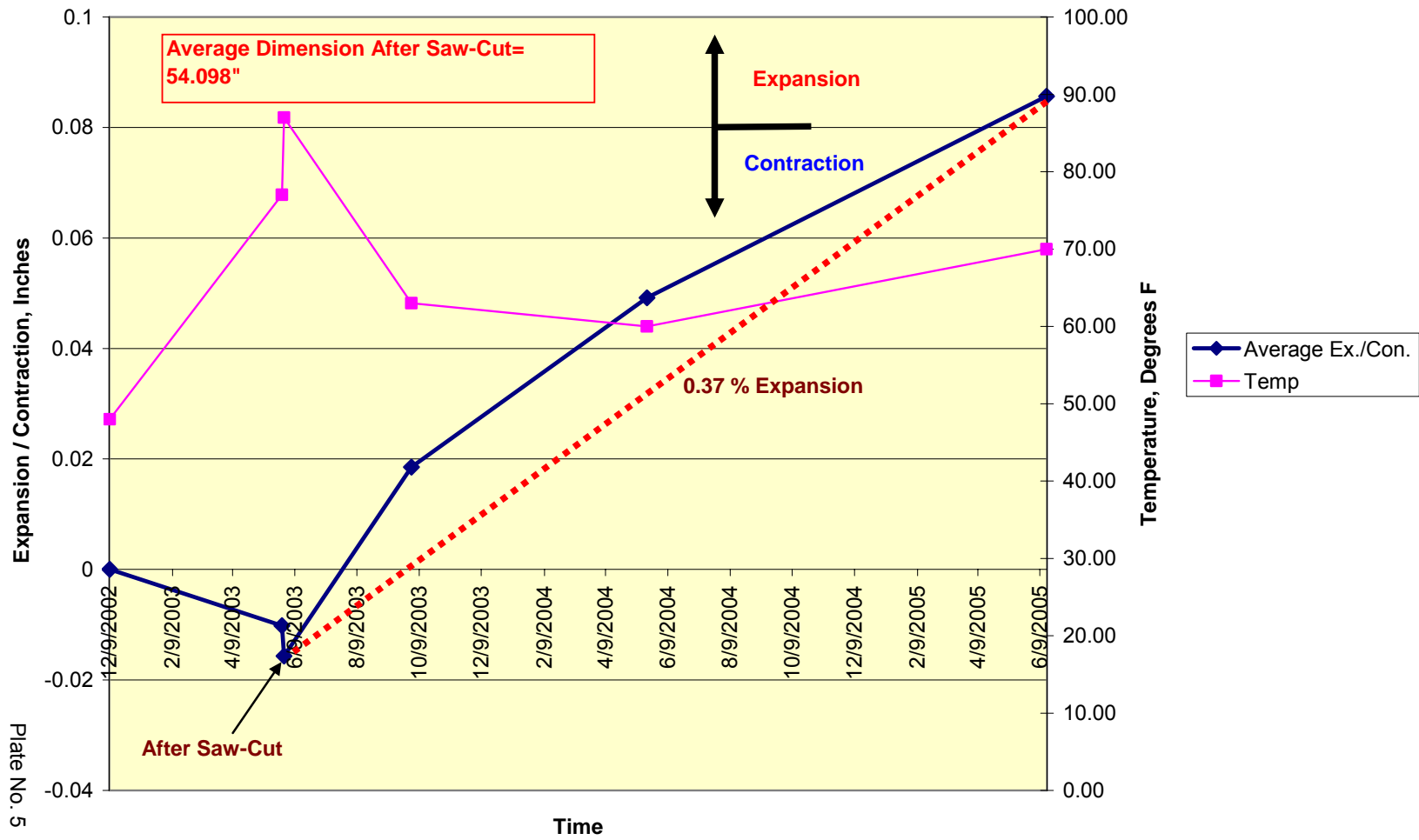
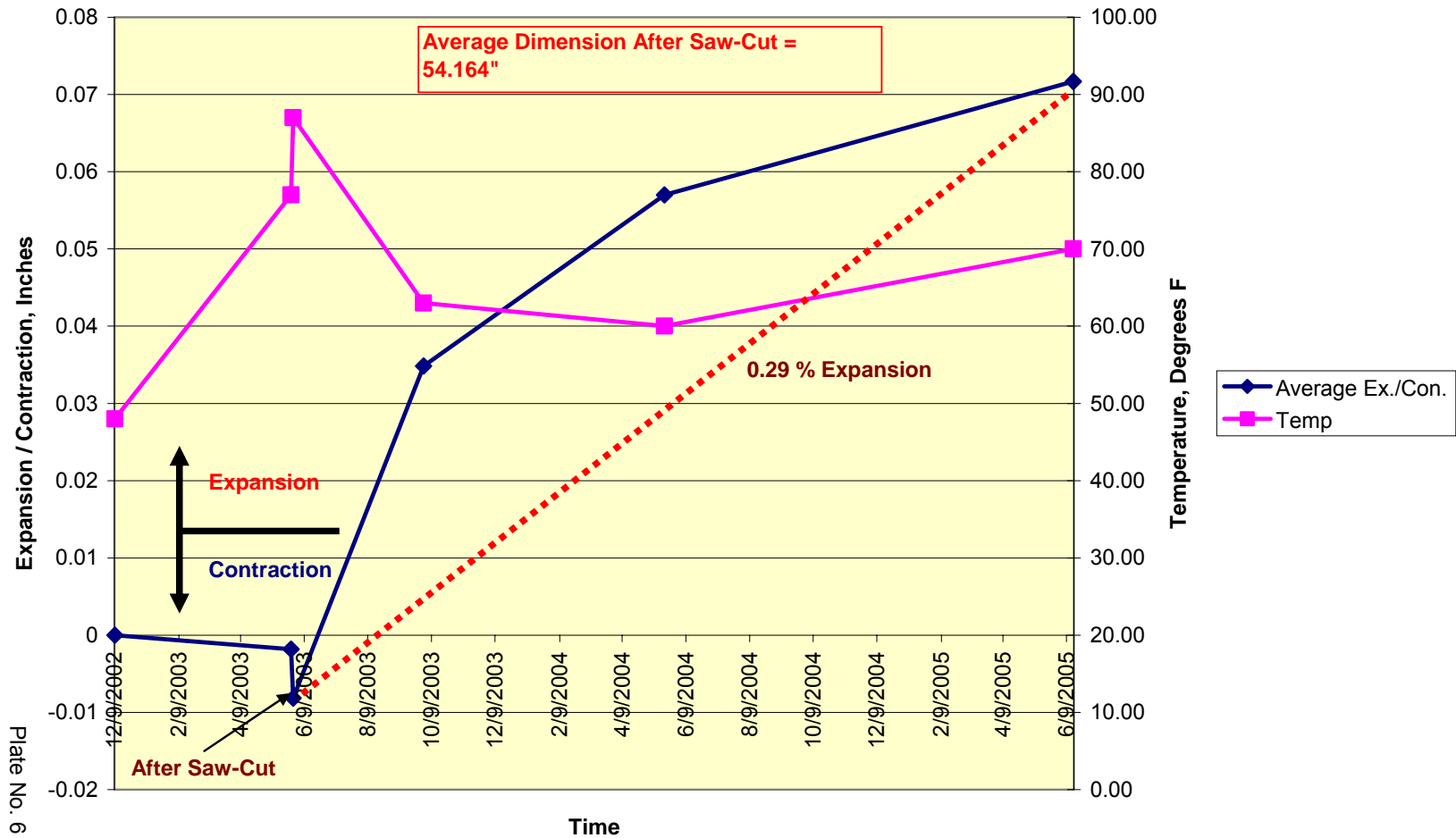


Plate No. 4

Panel No. 11A (Treated)  
Average East-West Movement

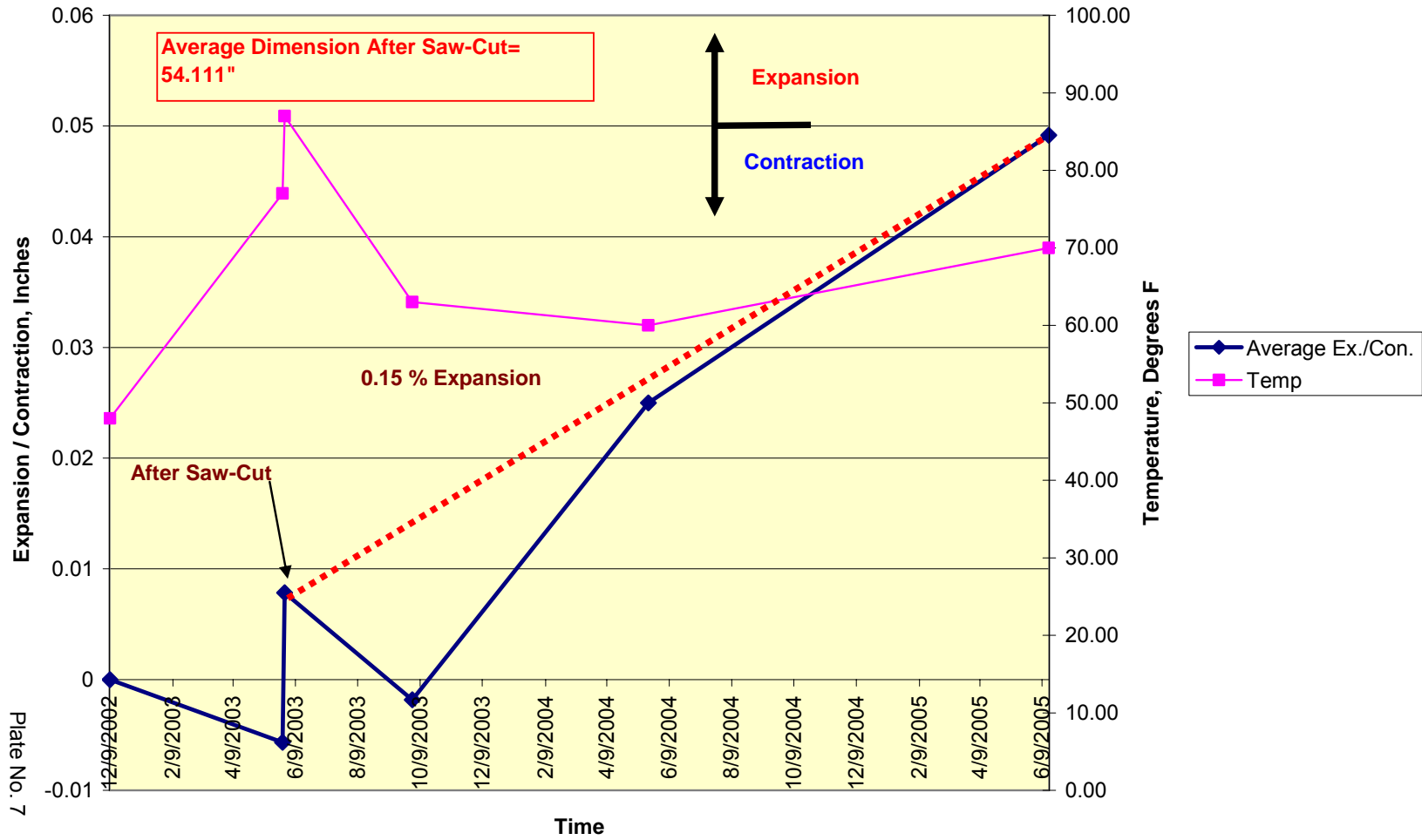


**Panel No. 11A (Treated)  
Average North - South Movement**

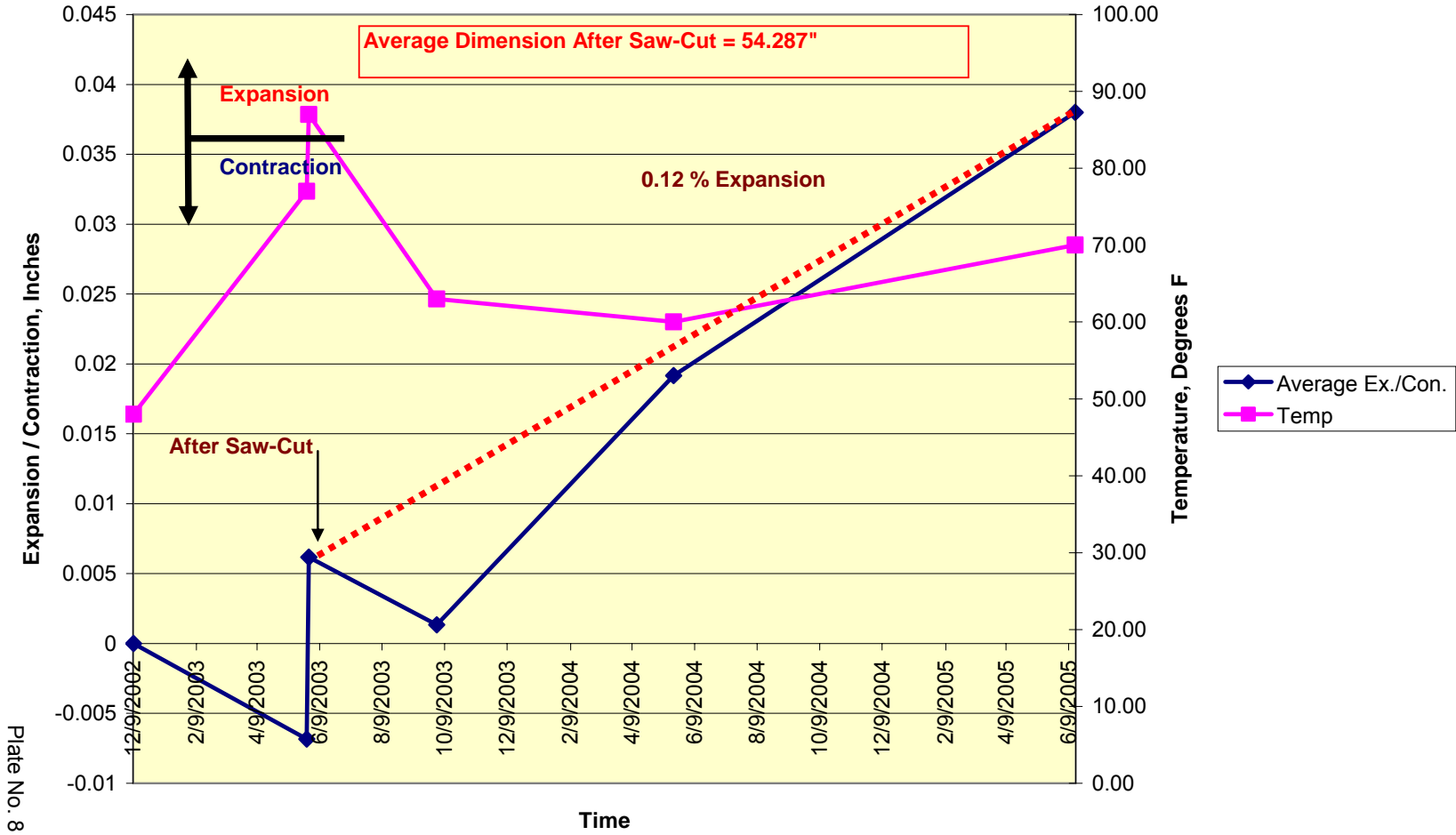




**Panel No. 14 (Control)**  
**Average East-West Movement**

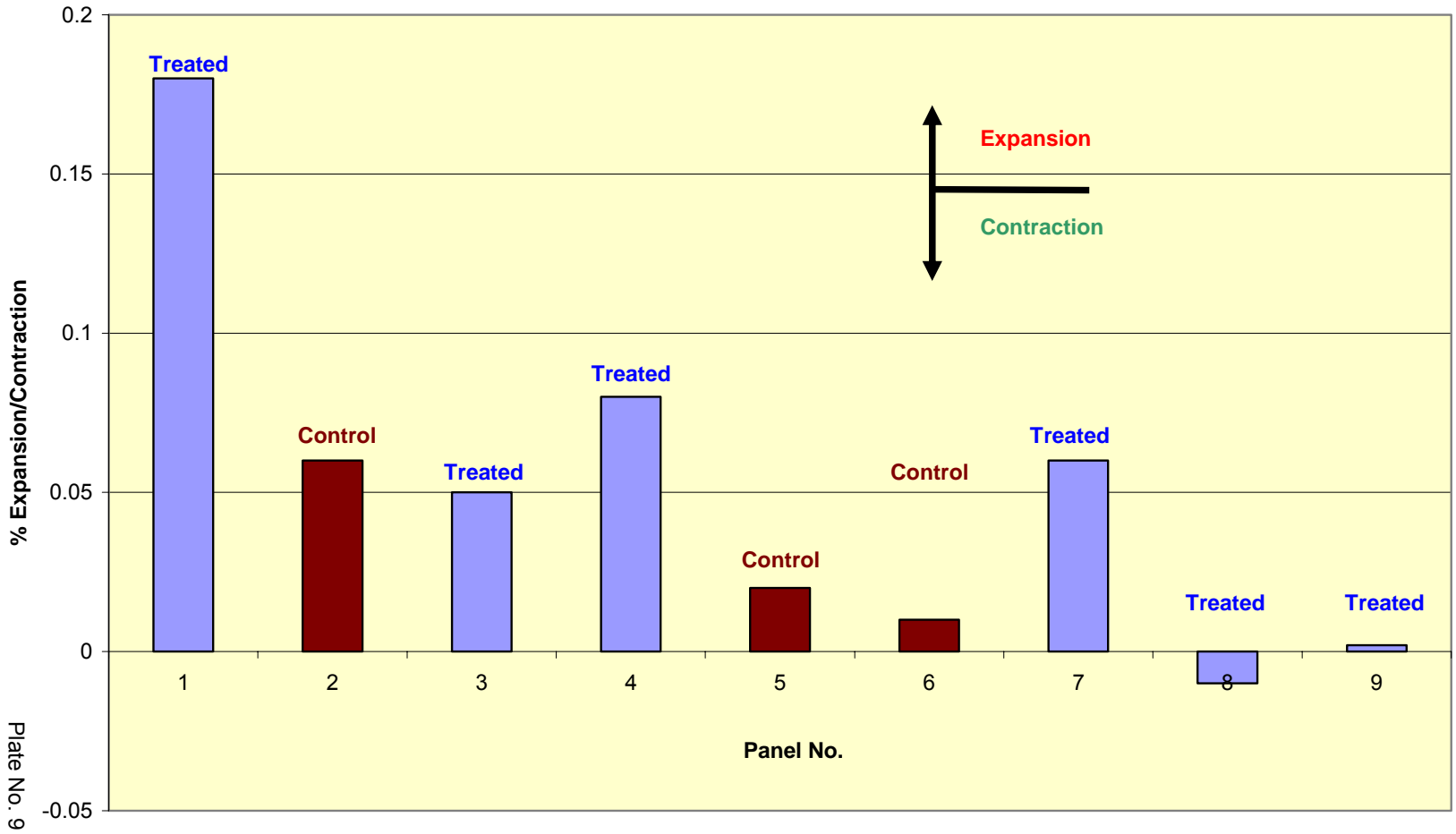


**Panel No. 14 (Control)**  
**Average North - South Movement**



8 Plate No. 8

### East-West Expansion Contraction New Concrete



### North-South Expansion Contraction New Concrete

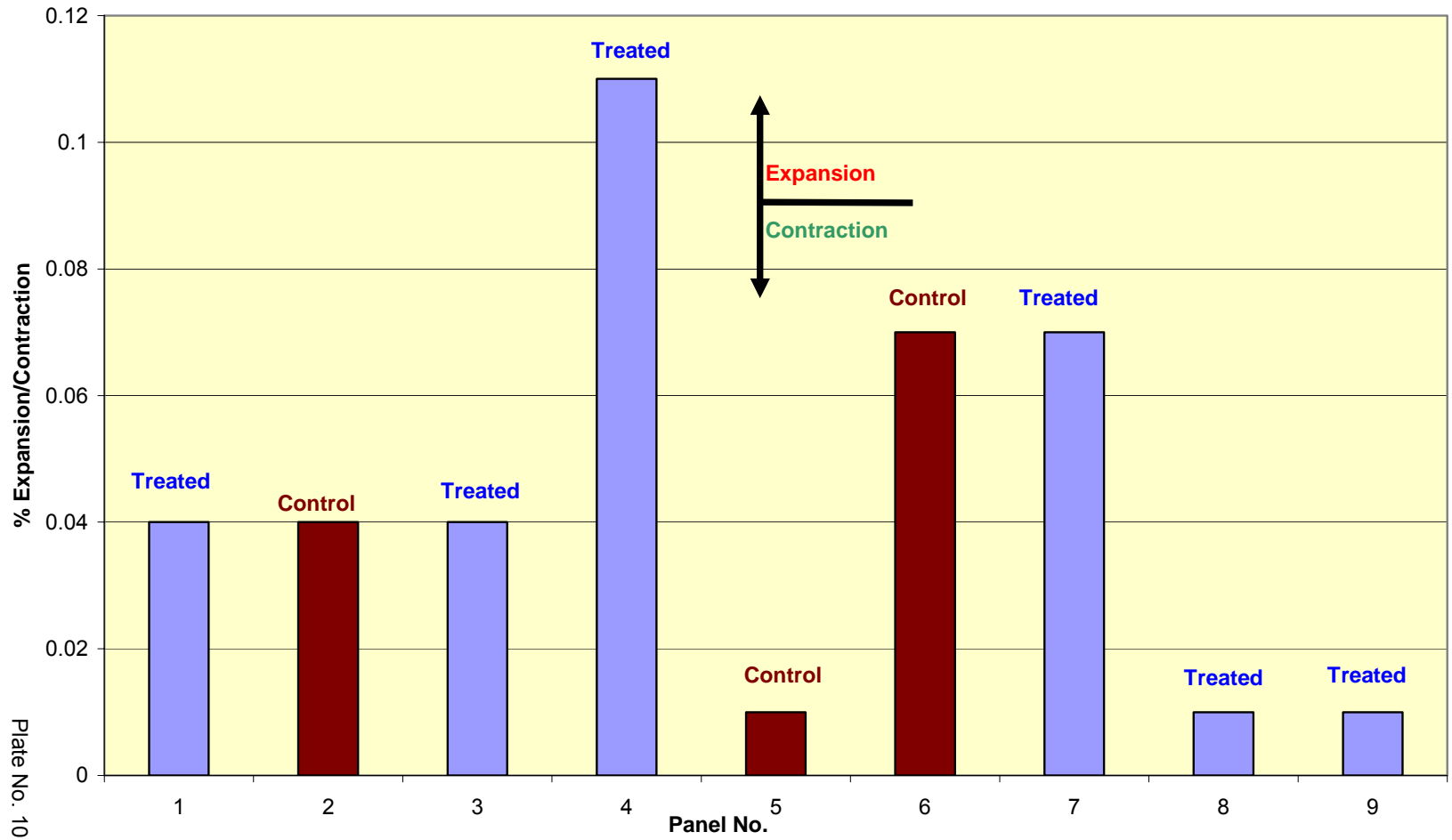


Plate No. 10

### East-West Expansion Contraction Old Concrete

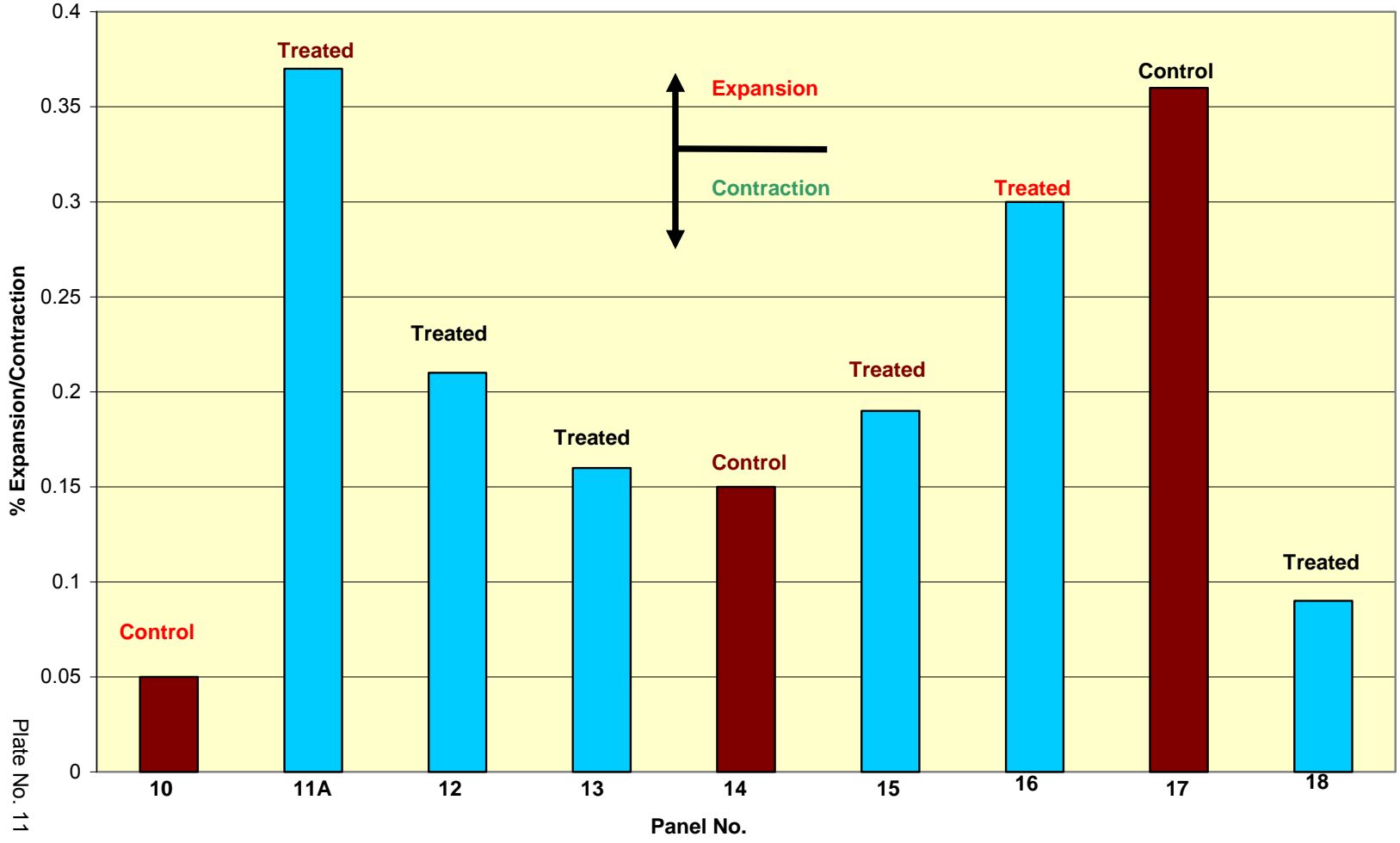


Plate No. 11

### North-South Expansion Contraction Old Concrete

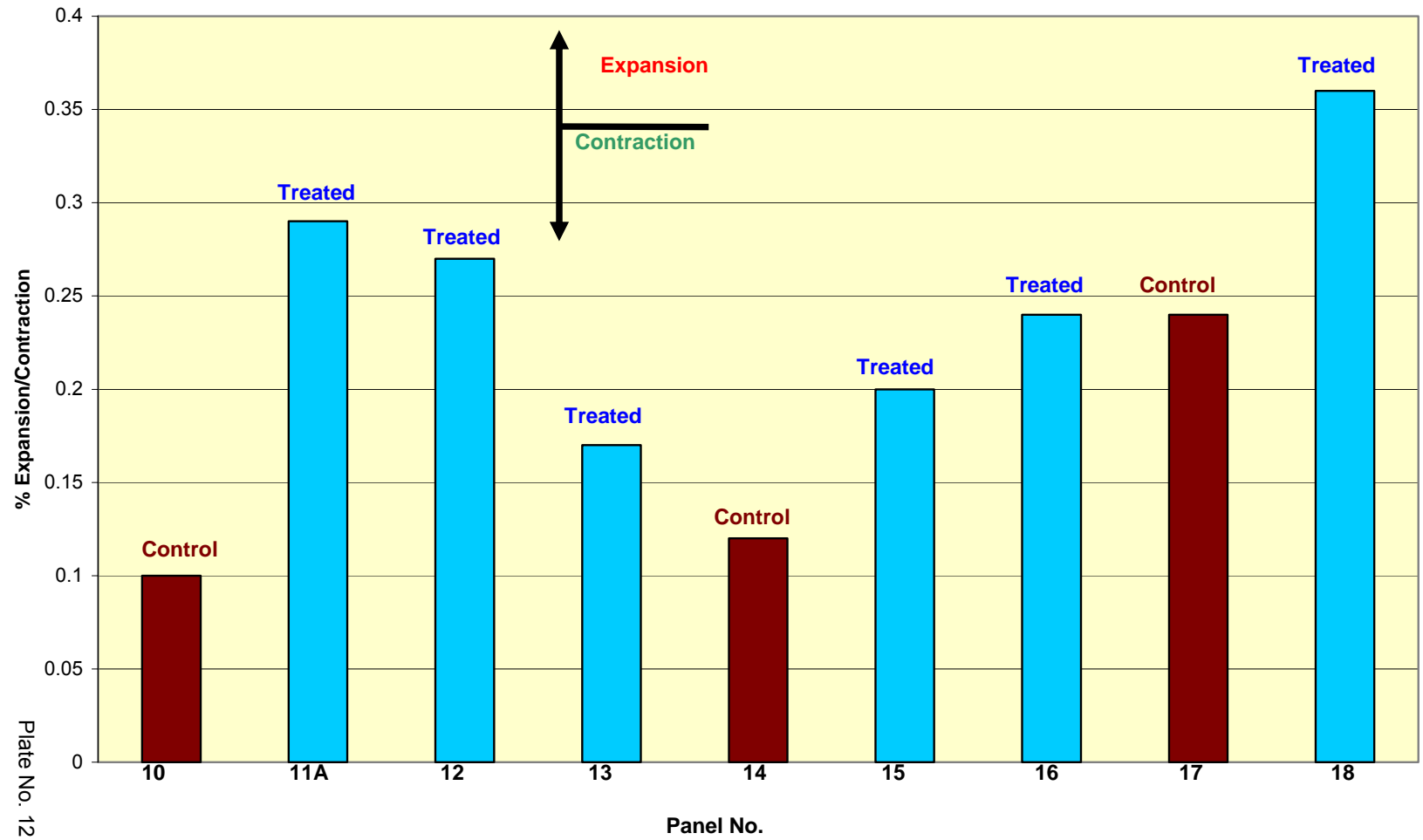


Plate No. 12

### East-West Expansion / Contraction

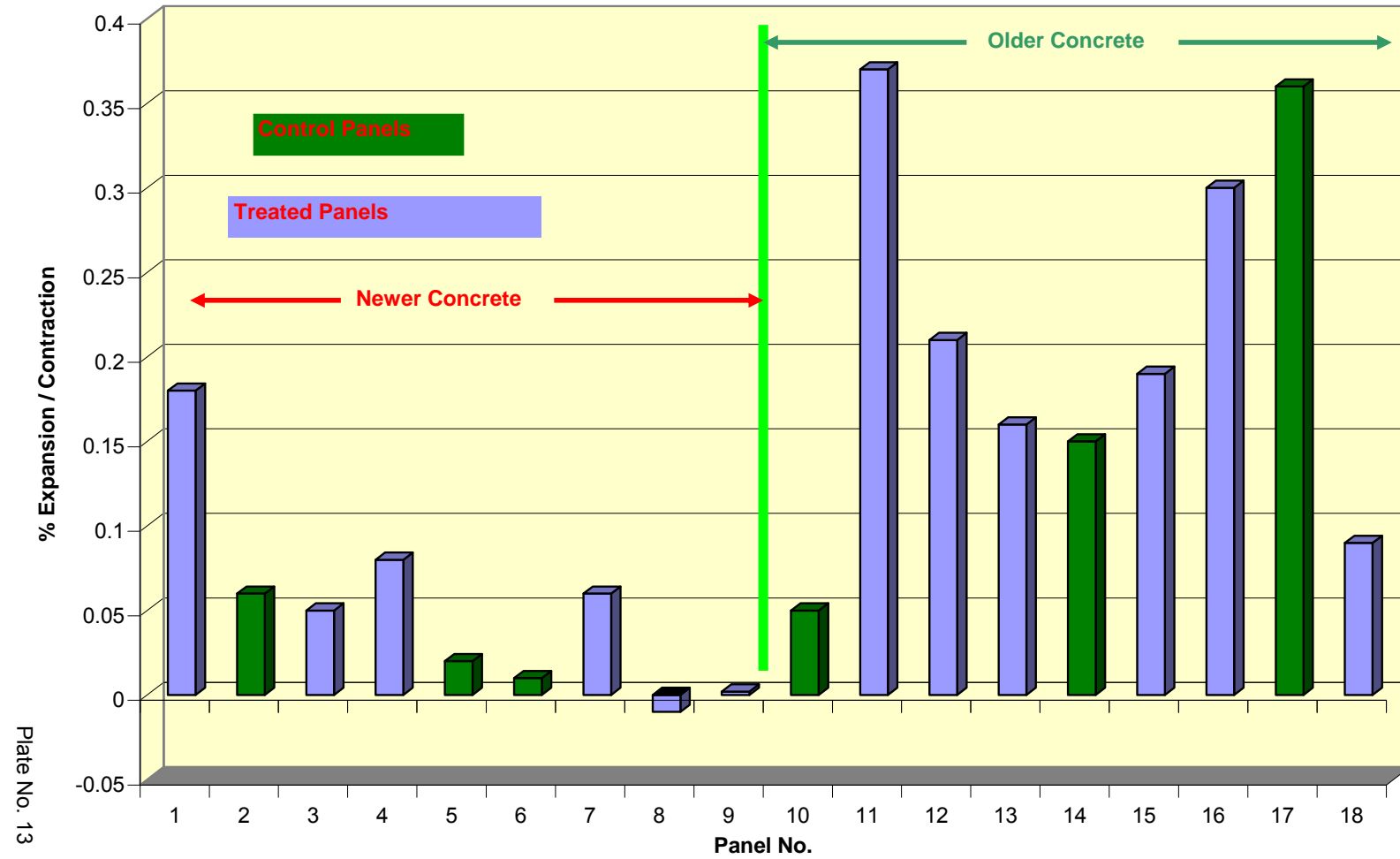


Plate No. 13

### North-South Expansion / Contraction

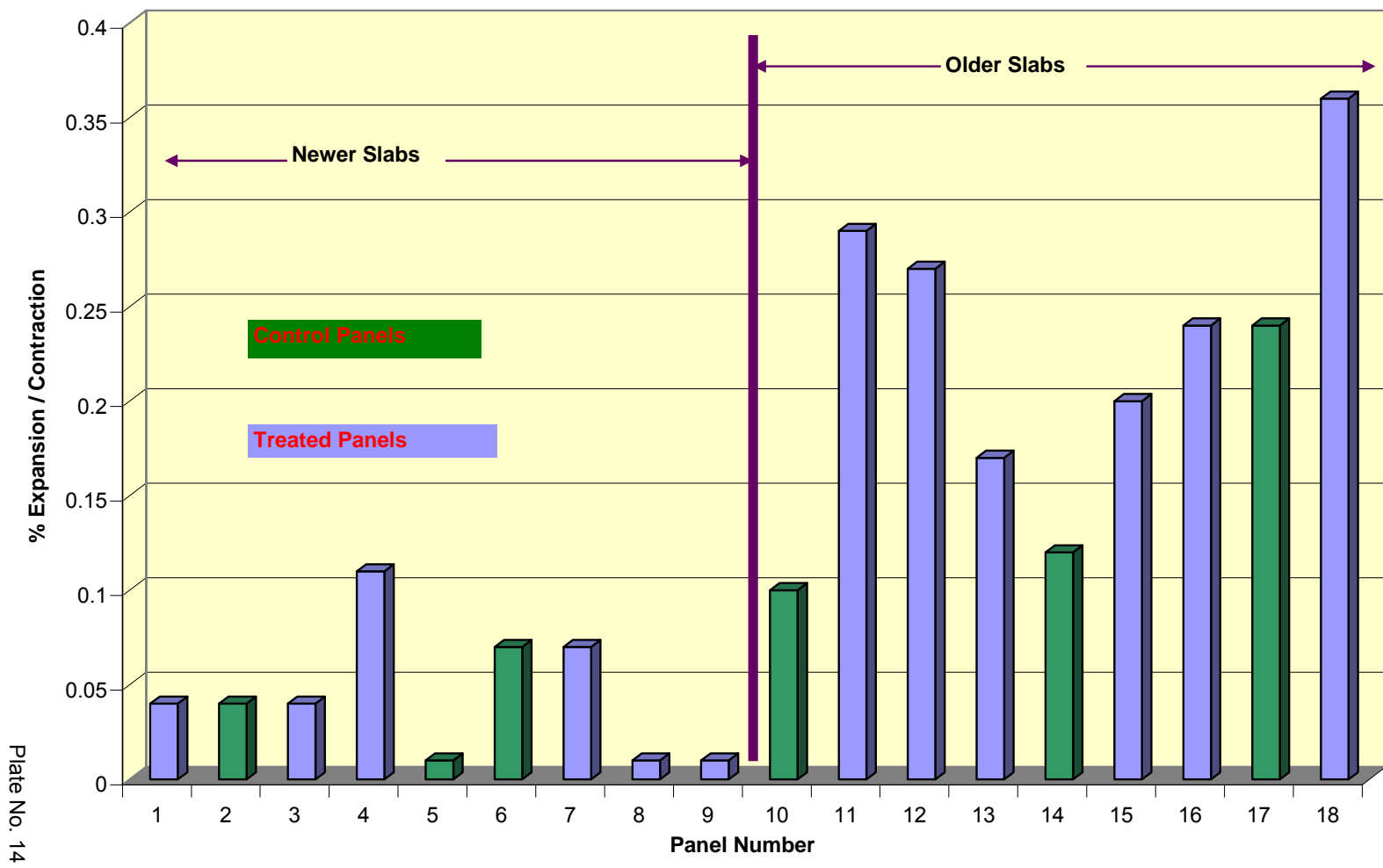
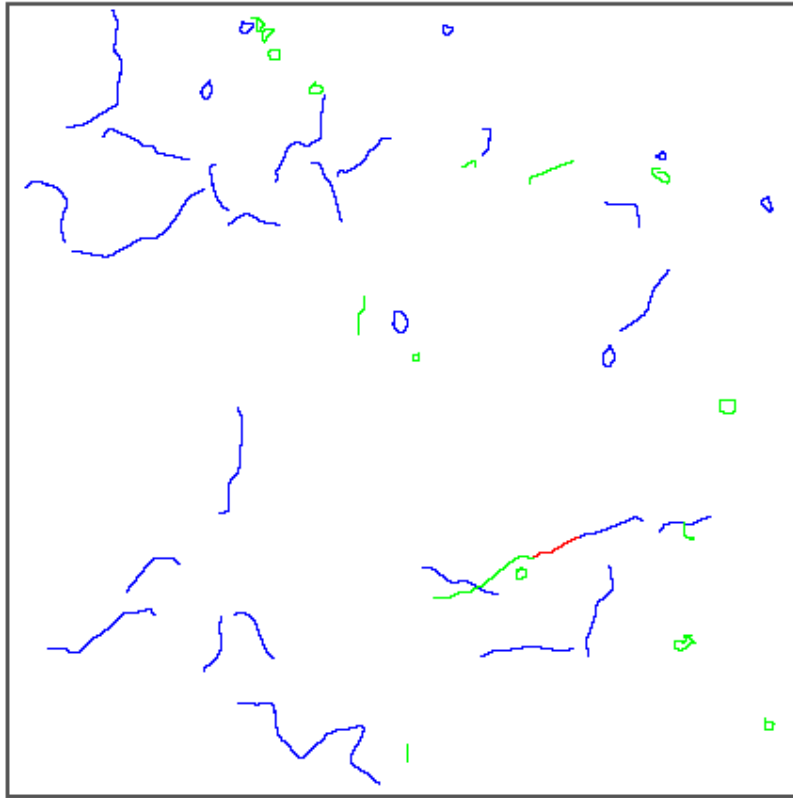


Plate No. 14



# **EXHIBIT NO. 2**

CDNTROL



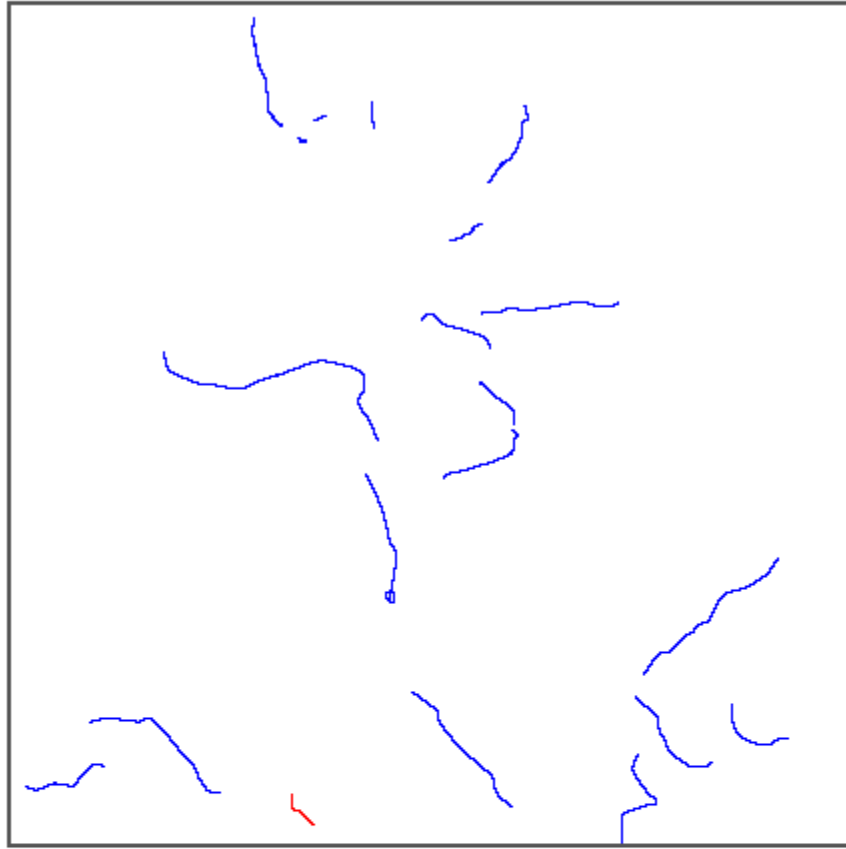
— JUNE 05  
— MAY 04  
— OCTOBER 02

PANEL 6 NO. 2



Plate No. 1

CONTRDL

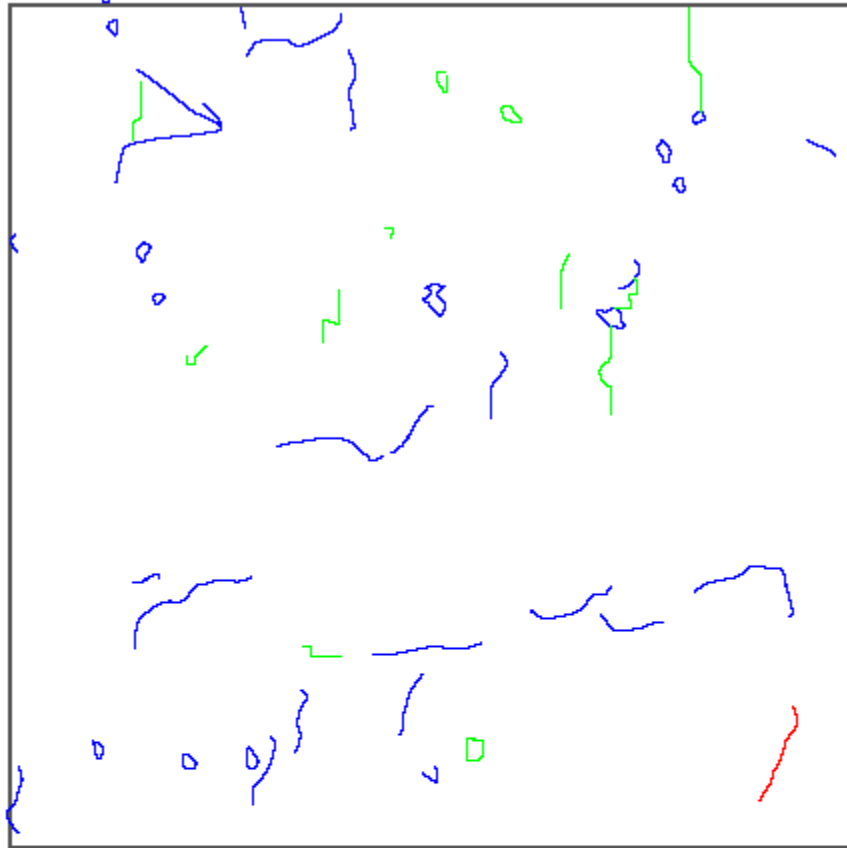


— JUNE 05  
— MAY 04  
— OCTOBER 02

PANEL 6 NO. 3 

Plate No. 2

CONTROL



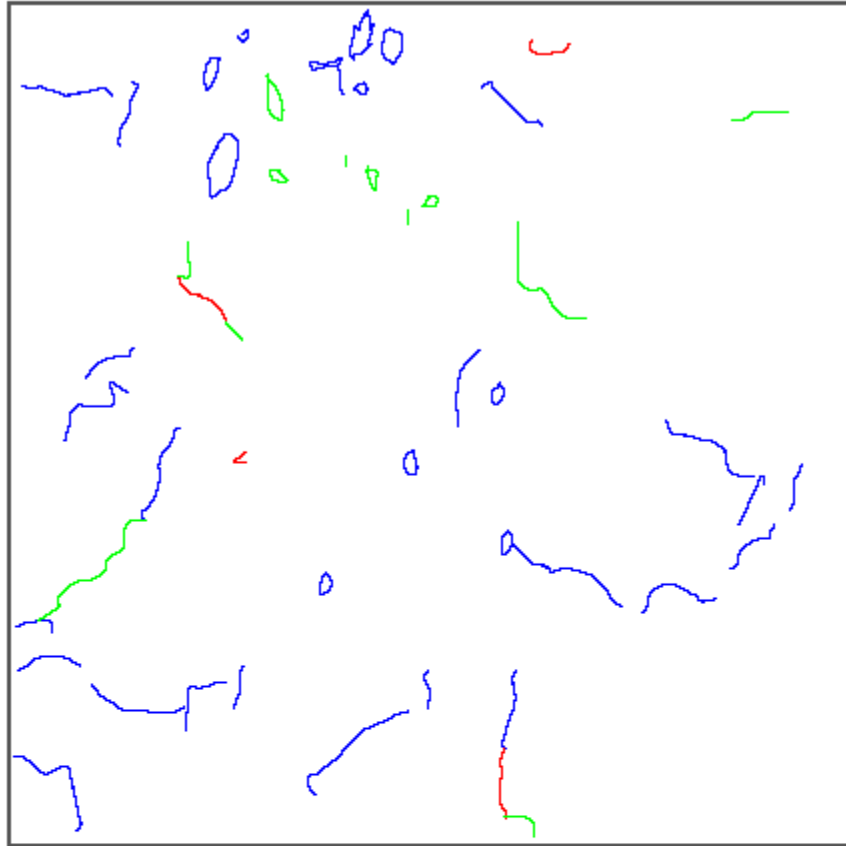
— JUNE 05  
— MAY 04  
— OCTOBER 02

PANEL 6 NO. 4



Plate No. 3

CONTROL



CONTROL

— JUNE 05

— MAY 04

— OCTOBER 02

PANEL 6 NO. 5

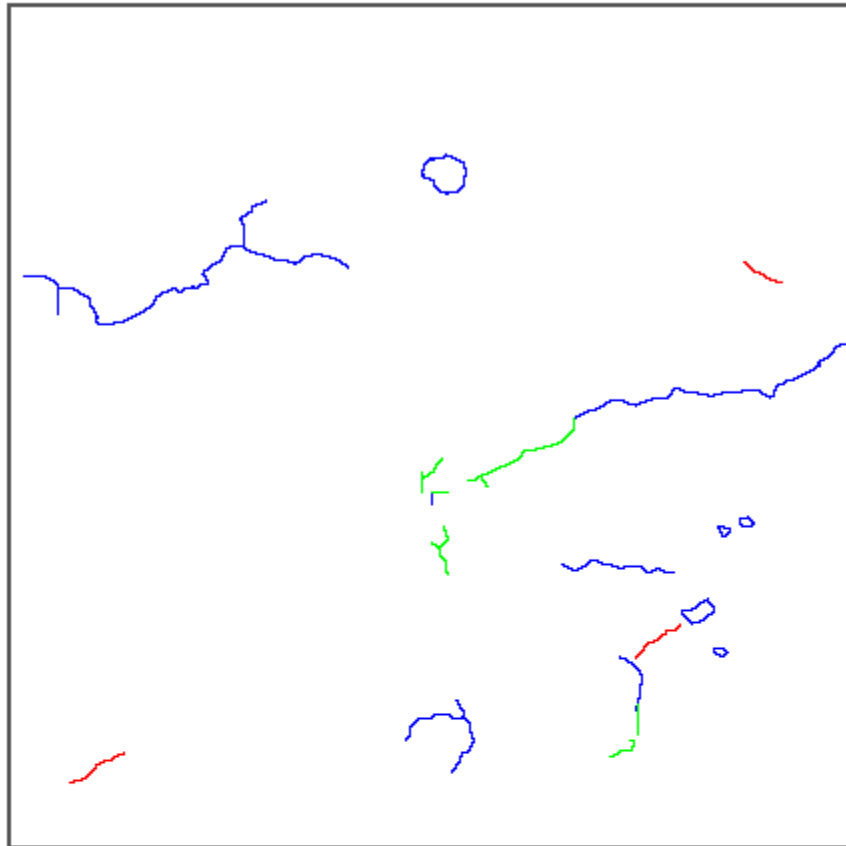


US Army Corps  
of Engineers  
Omaha District



Plate No. 4

TREATED



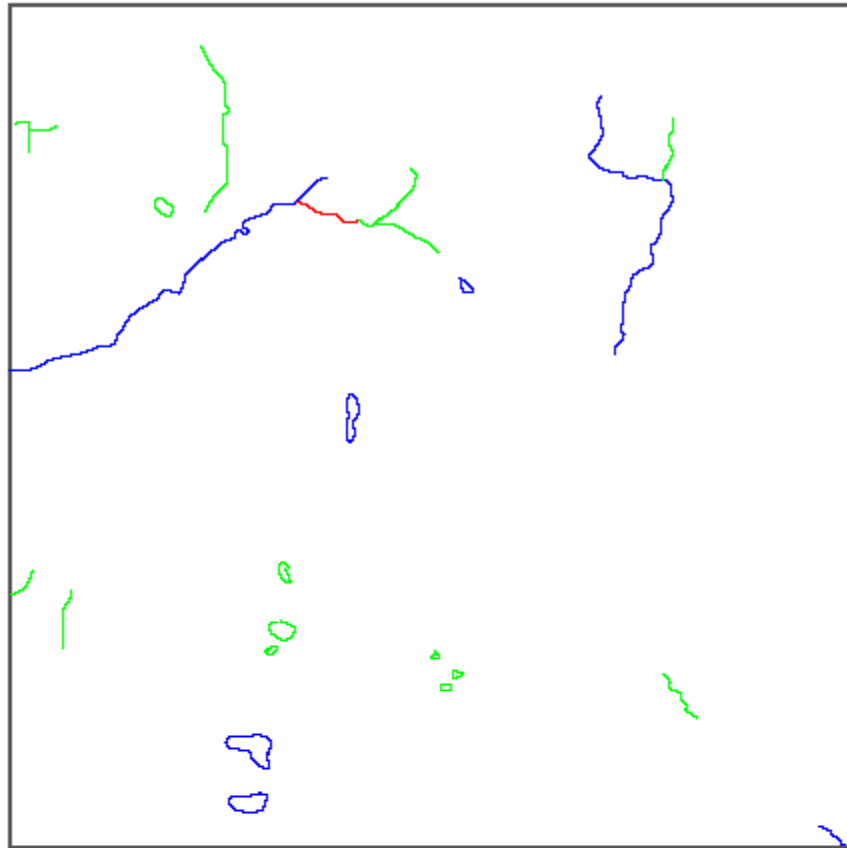
— JUNE 05  
— MAY 04  
— OCTOBER 02

PANEL 7 NO. 1



PLATE NO. 5

TREATED



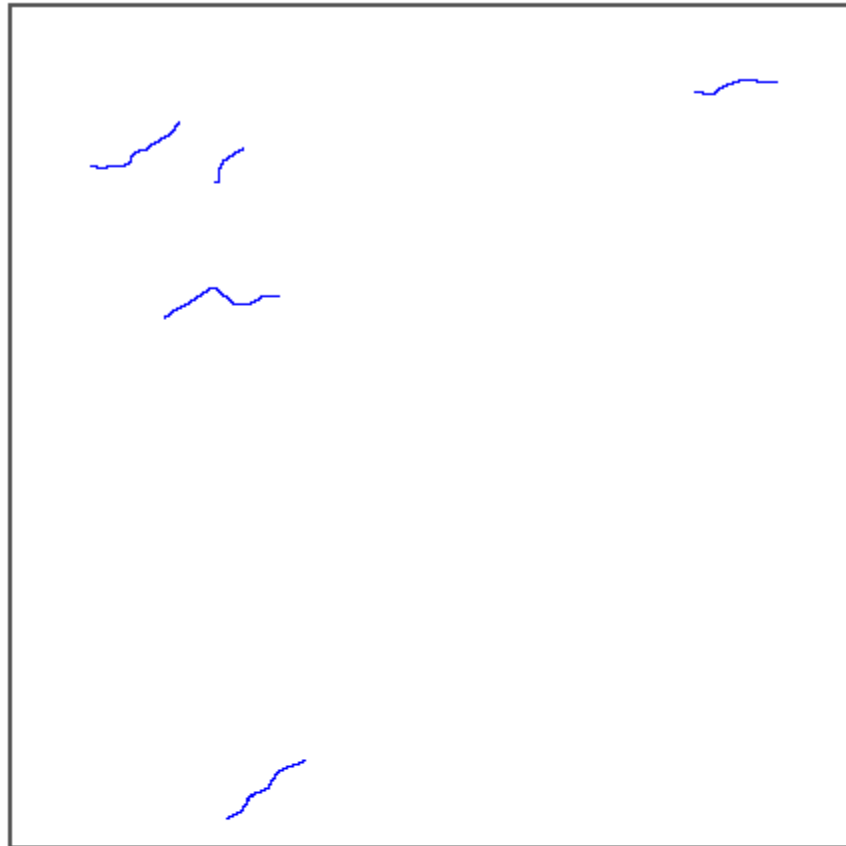
— JUNE 05  
— MAY 04  
— OCTOBER 02

PANEL 7 NO. 2



PLATE NO. 6

TREATED



— JUNE 05

— MAY 04

— OCTOBER 02

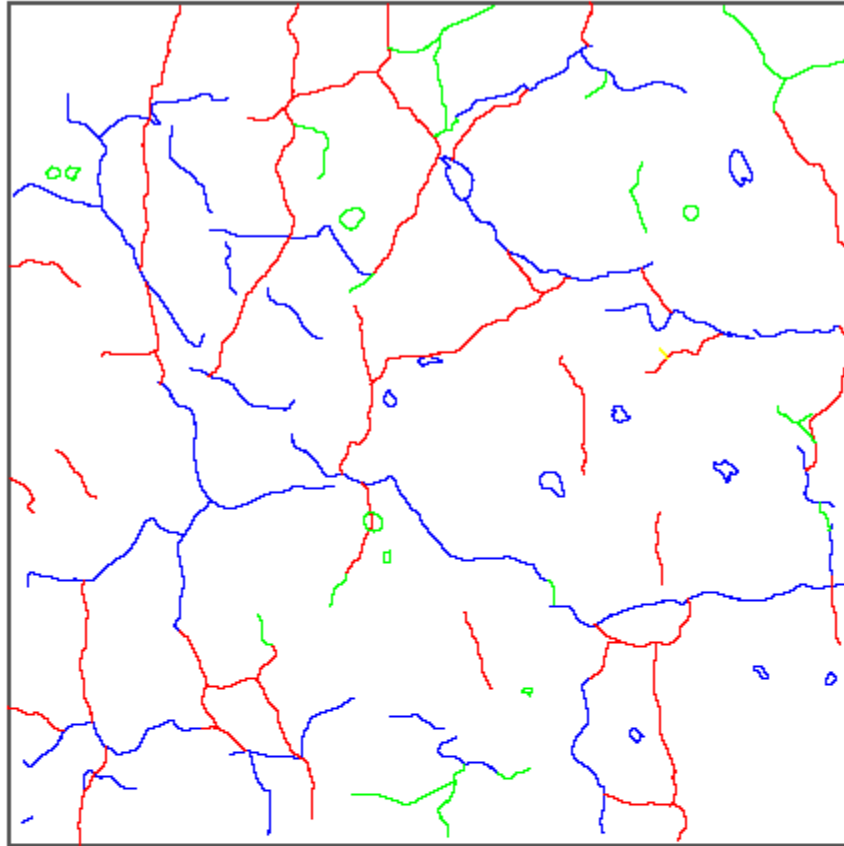
PANEL 7 NO. 3



PLATE NO. 7



CONTROL



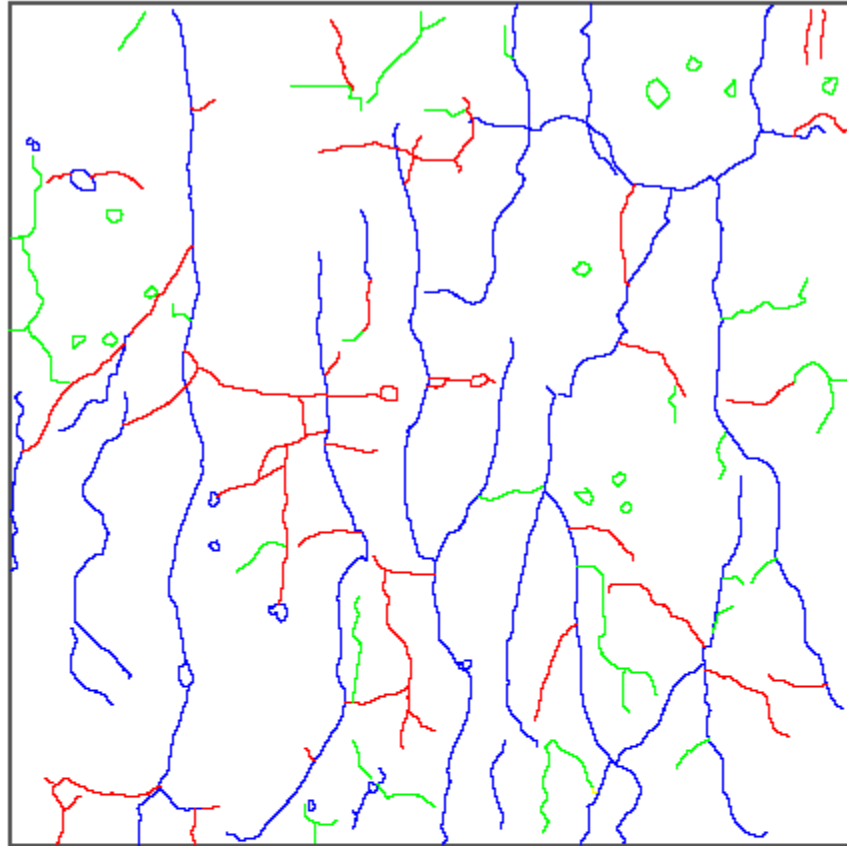
— JUNE 05  
— MAY 04  
— OCTOBER 02

PANEL 17 NO. 1



PLATE NO. 8

CONTROL



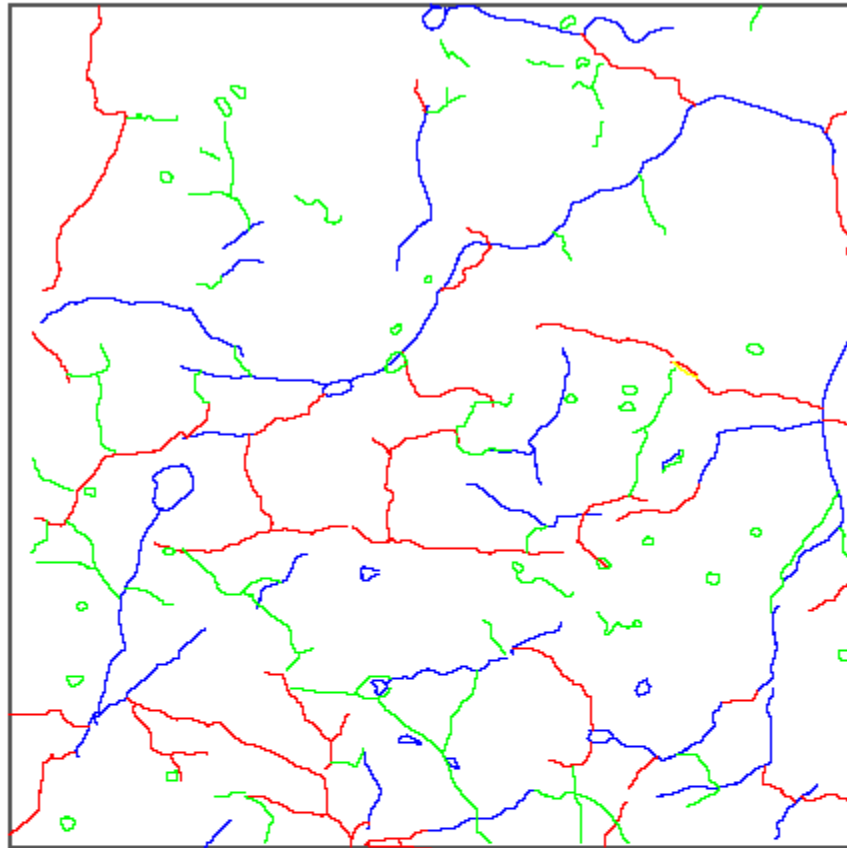
— JUNE 05  
— MAY 04  
— OCTOBER 02

PANEL 17 NO. 2



PLATE NO. 9

CDNTROL



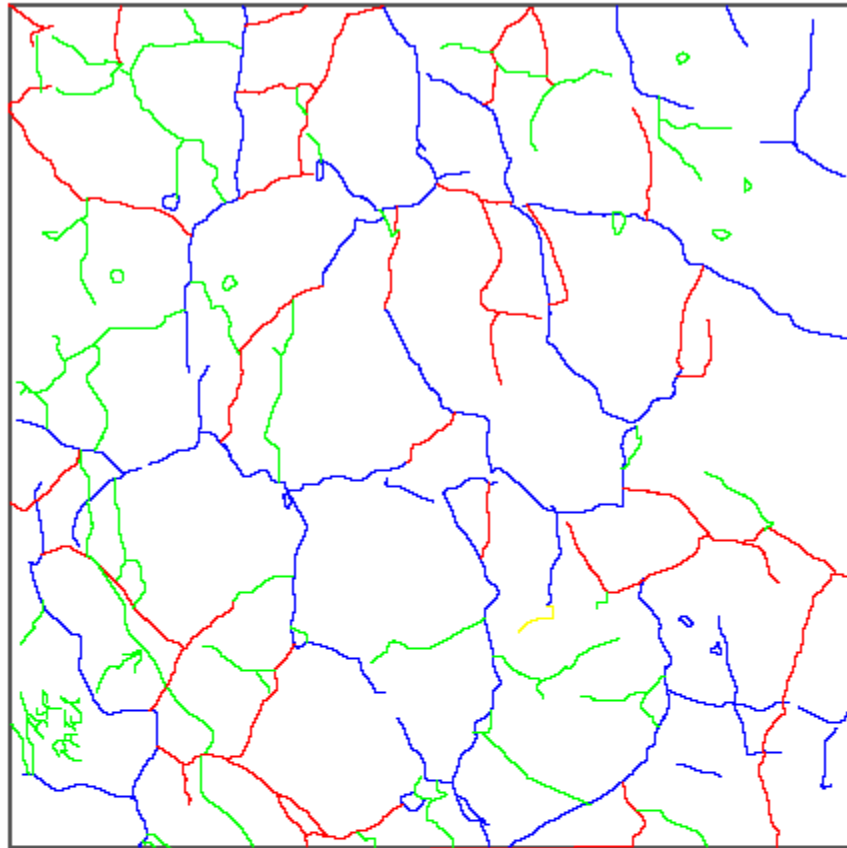
— JUNE 05  
— MAY 04  
— OCTOBER 02

PANEL 17 NO. 3



PLATE NO. 10

CONTROL



— JUNE 05  
— MAY 04  
— OCTOBER 02

PANEL 17 NO. 4



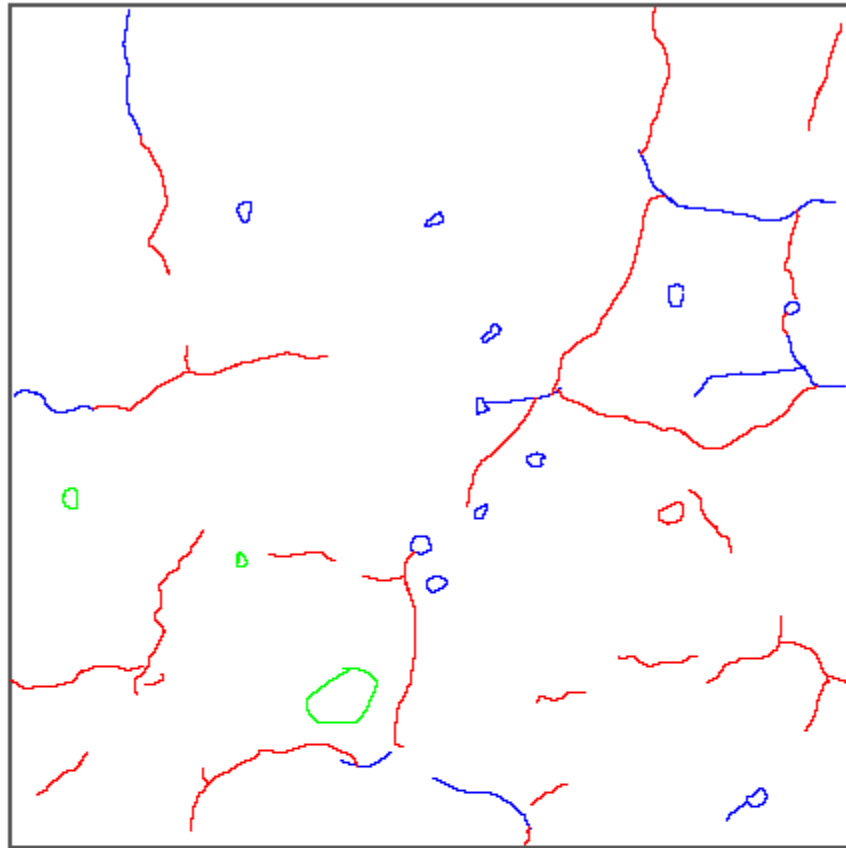
US Army Corps  
of Engineers  
Omaha District

UNIVERSITY OF  
**Nebraska**  
Lincoln

Nebraska  
Department of Roads

PLATE NO. 11

TREATED



— JUNE 05  
— MAY 04  
— OCTOBER 02



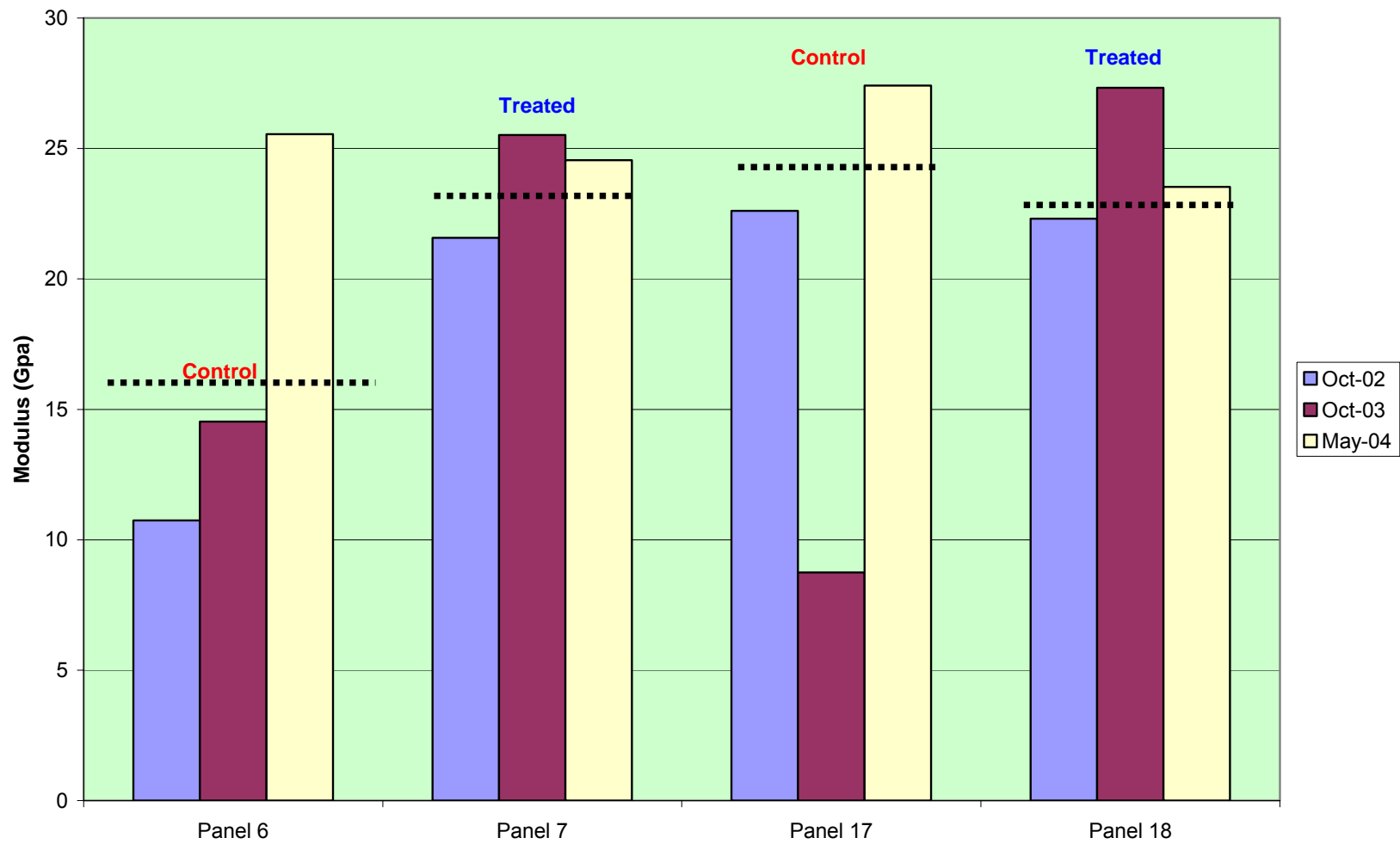
PANEL 18 NO. 3



PLATE NO. 12

# **EXHIBIT NO. 3**

### Impact Echo Data Evaluation



# **EXHIBIT NO. 4**



### Schmidt Hammer Evaluation

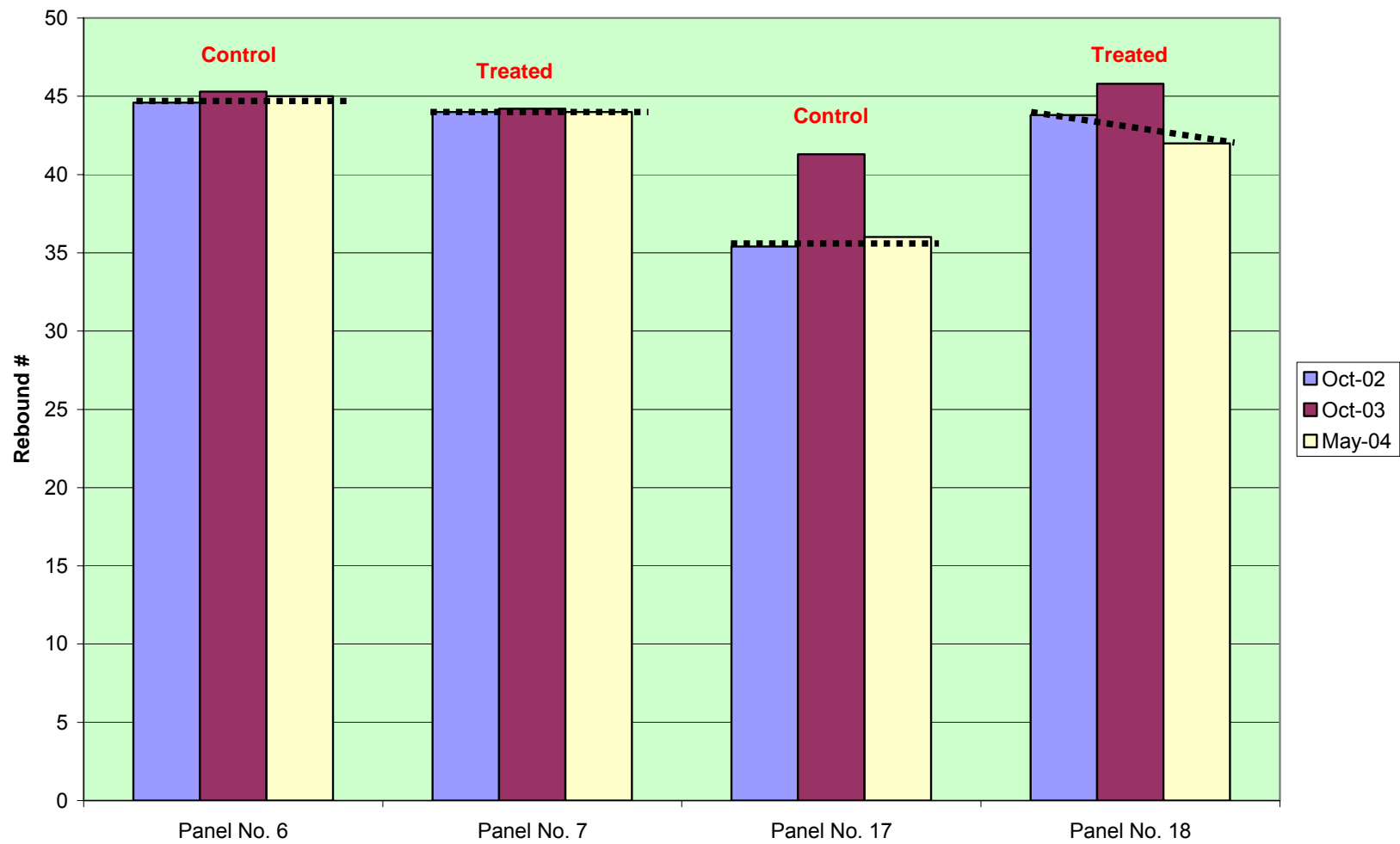


# **EXHIBIT NO. 5**

### V-Meter Data Evaluation

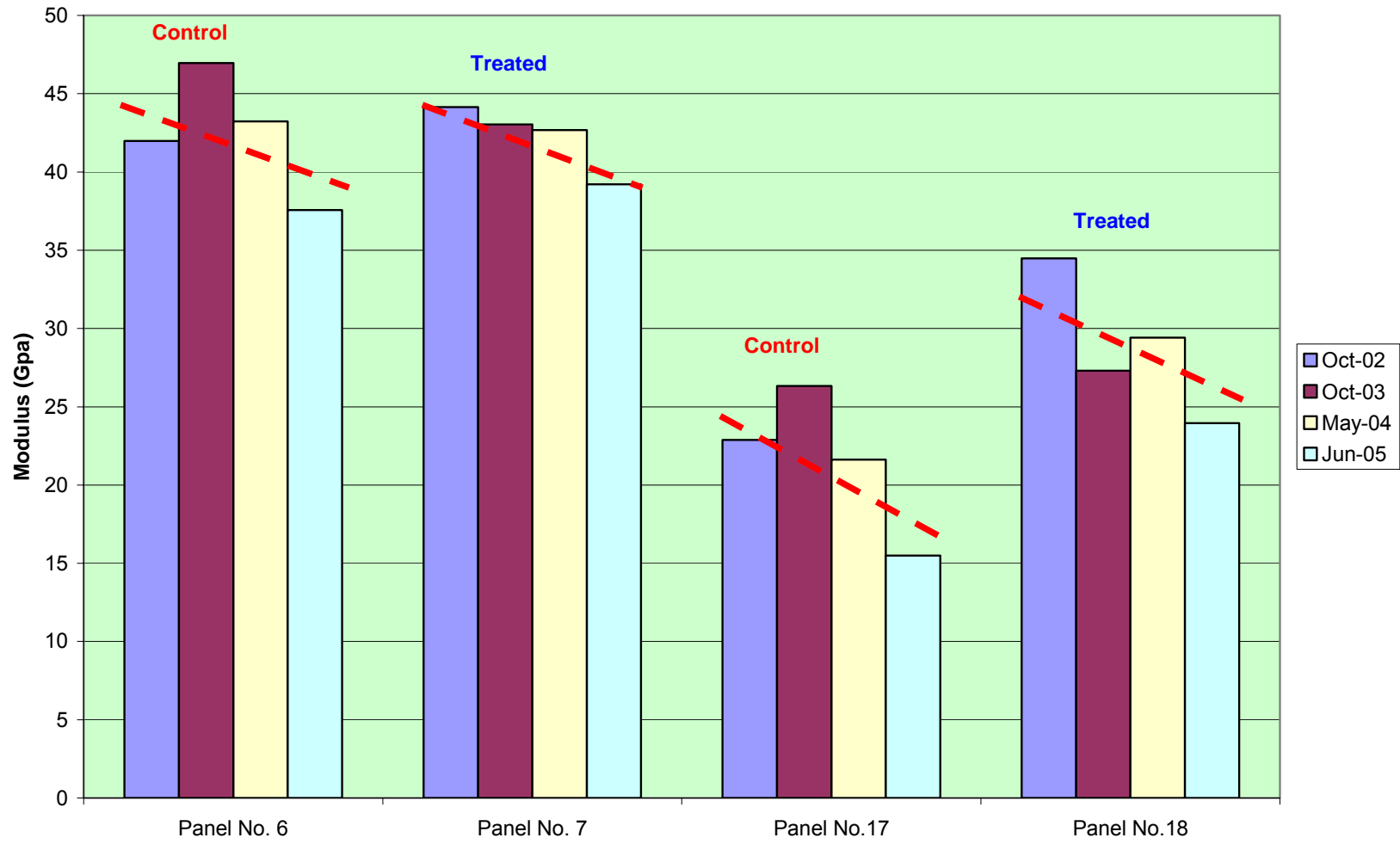
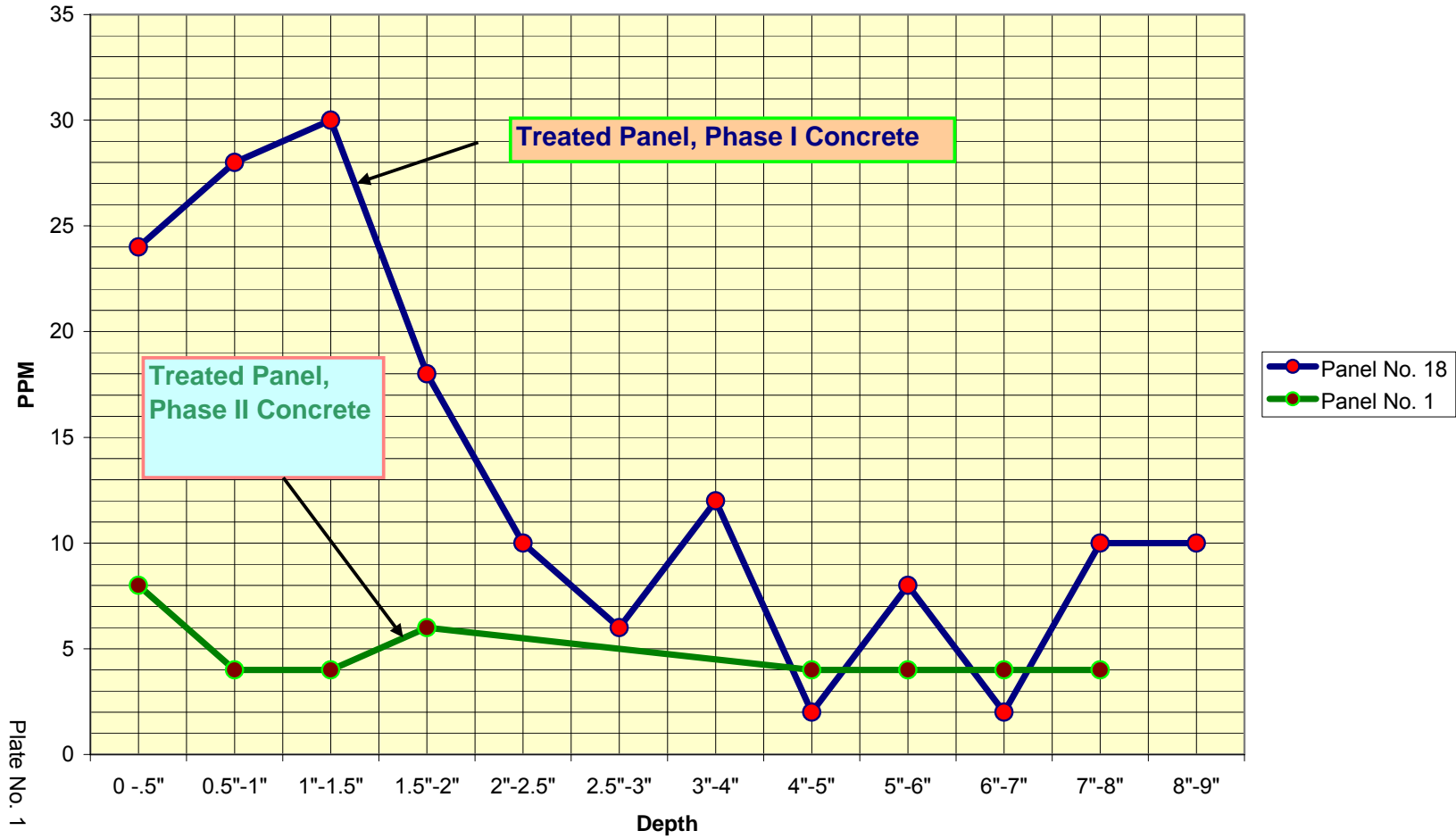
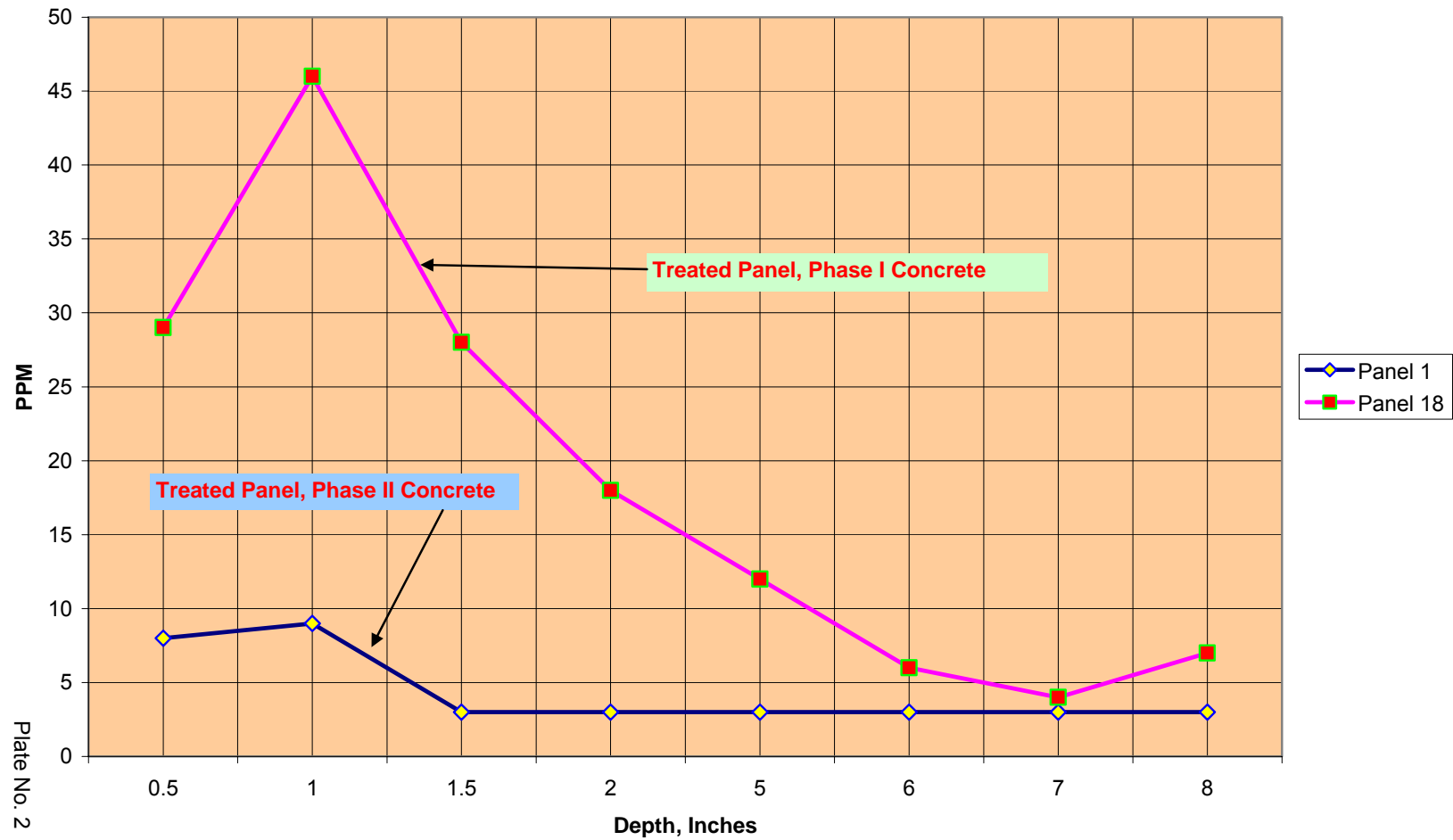


# **EXHIBIT NO. 6**

Lithium Content by Gravity Soaking  
October 2003



### Lithium Content by Gravity Soaking June 2005



Lithium Content  
Flood Coat  
Old Concrete vs. New Concrete

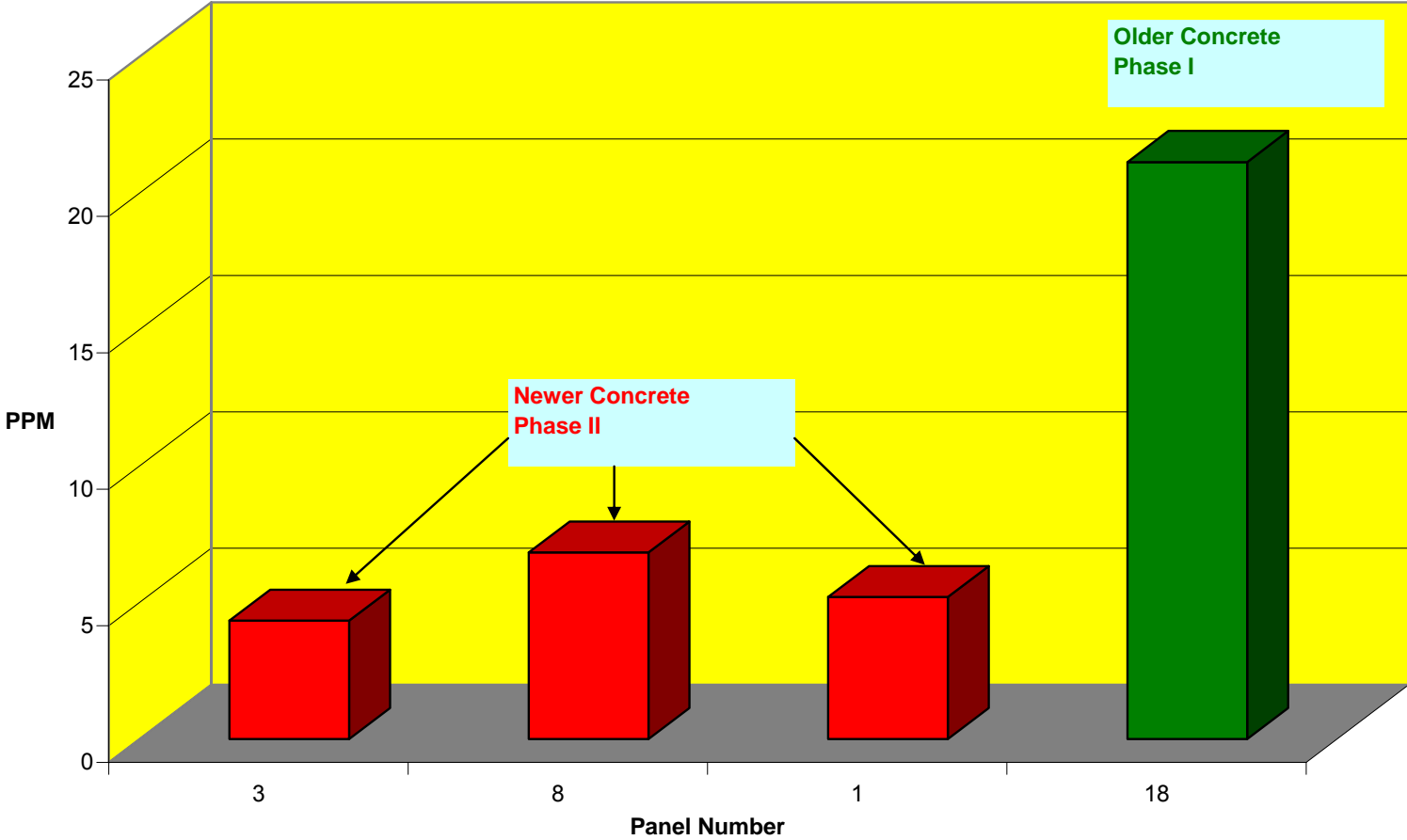


Plate No. 3

Lithium Content  
Panel No. 17  
Control

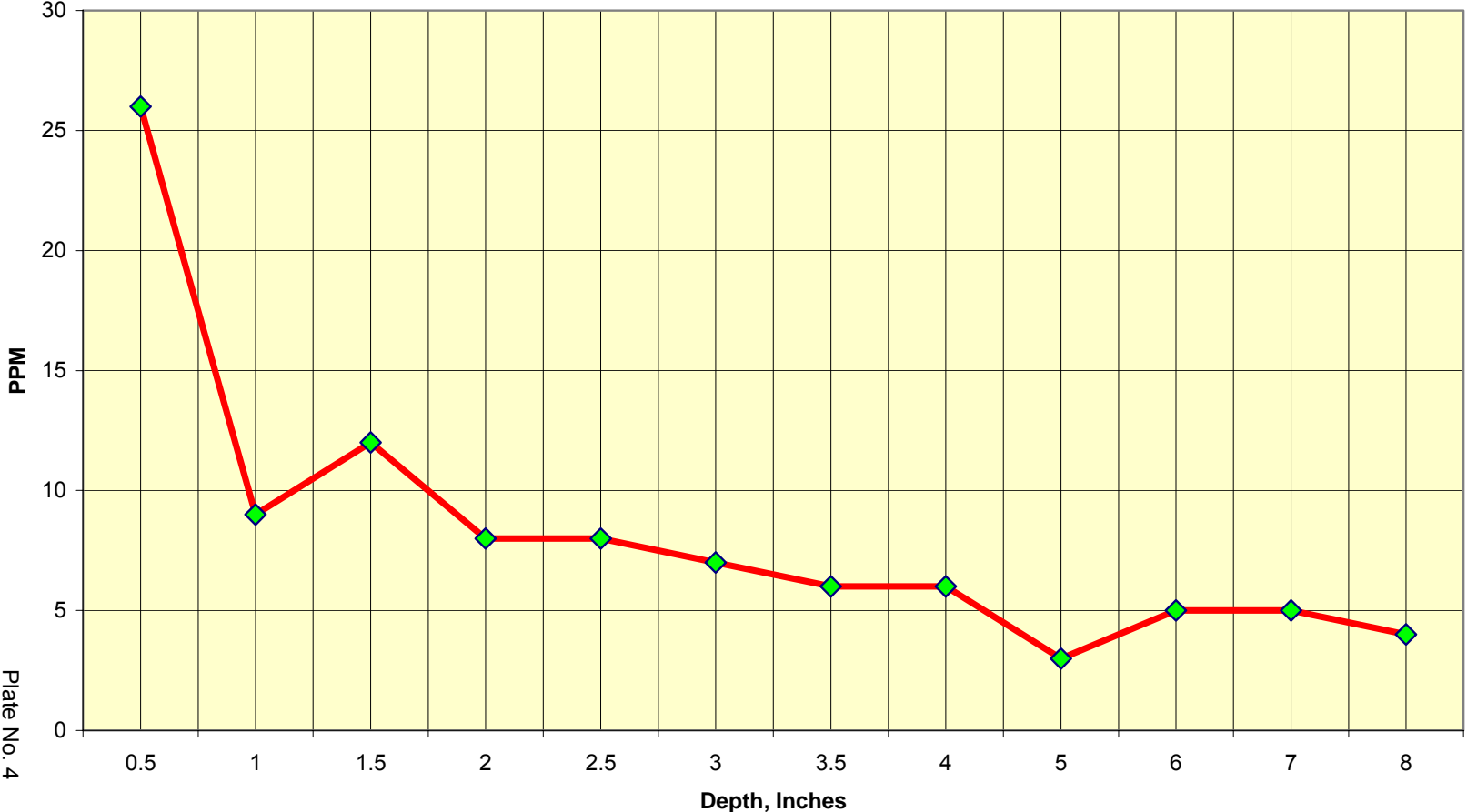


Plate No. 4



**Lithium Content  
Panel No. 13  
Pressure Treated**

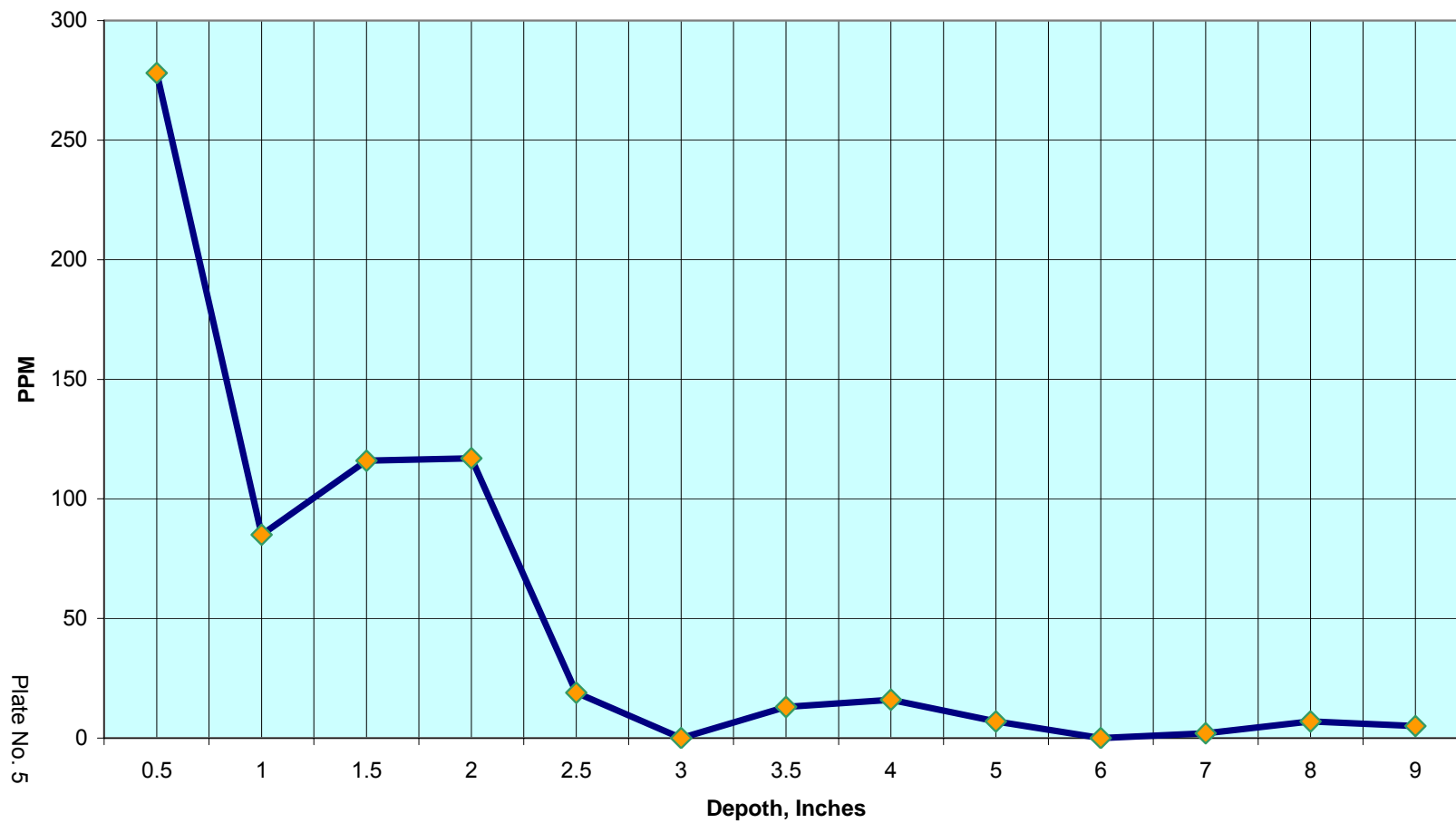


Plate No. 5

**Lithium Content  
Panel No. 15-1  
Vacuum Impregnation**

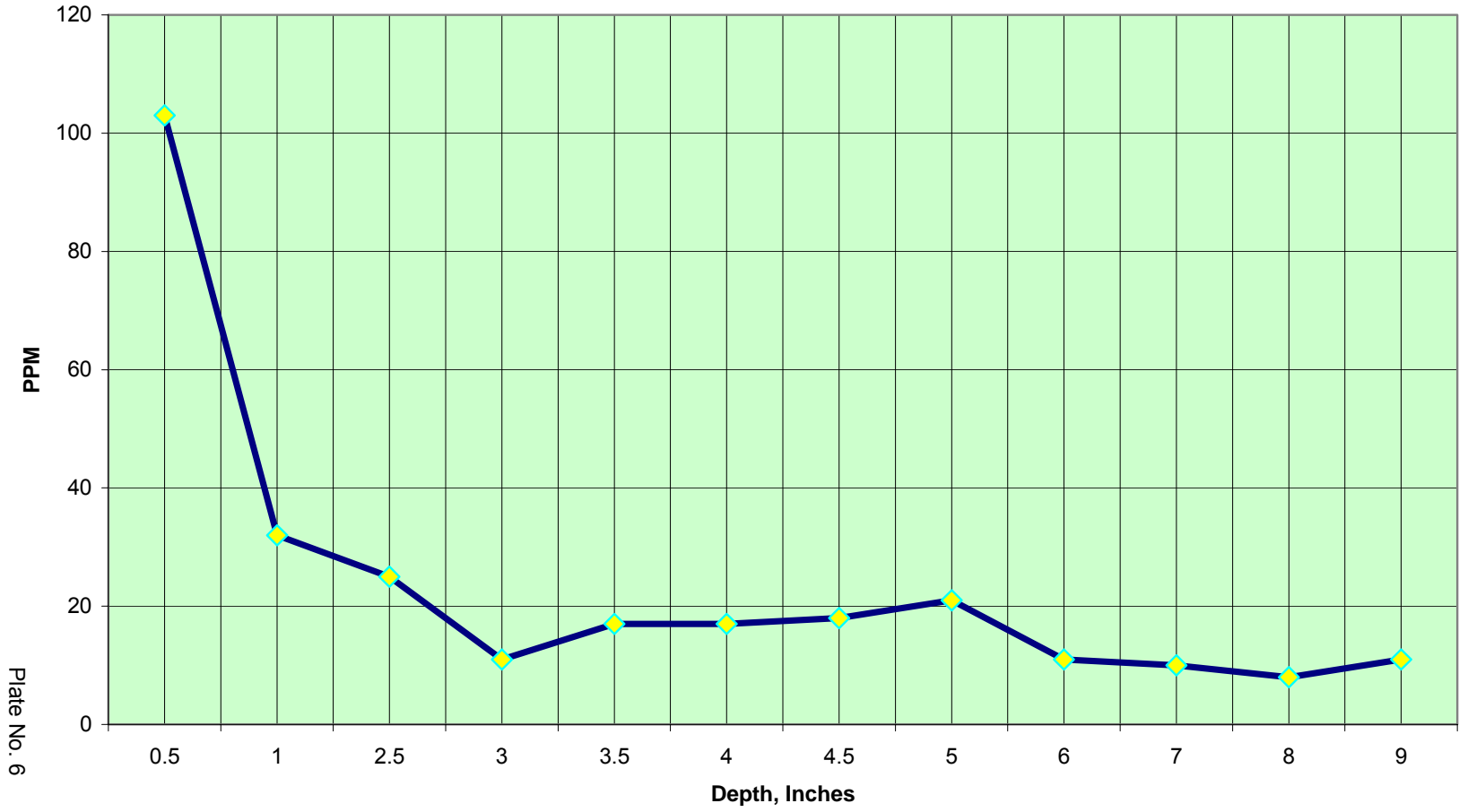


Plate No. 6

### Maximum Lithium Content

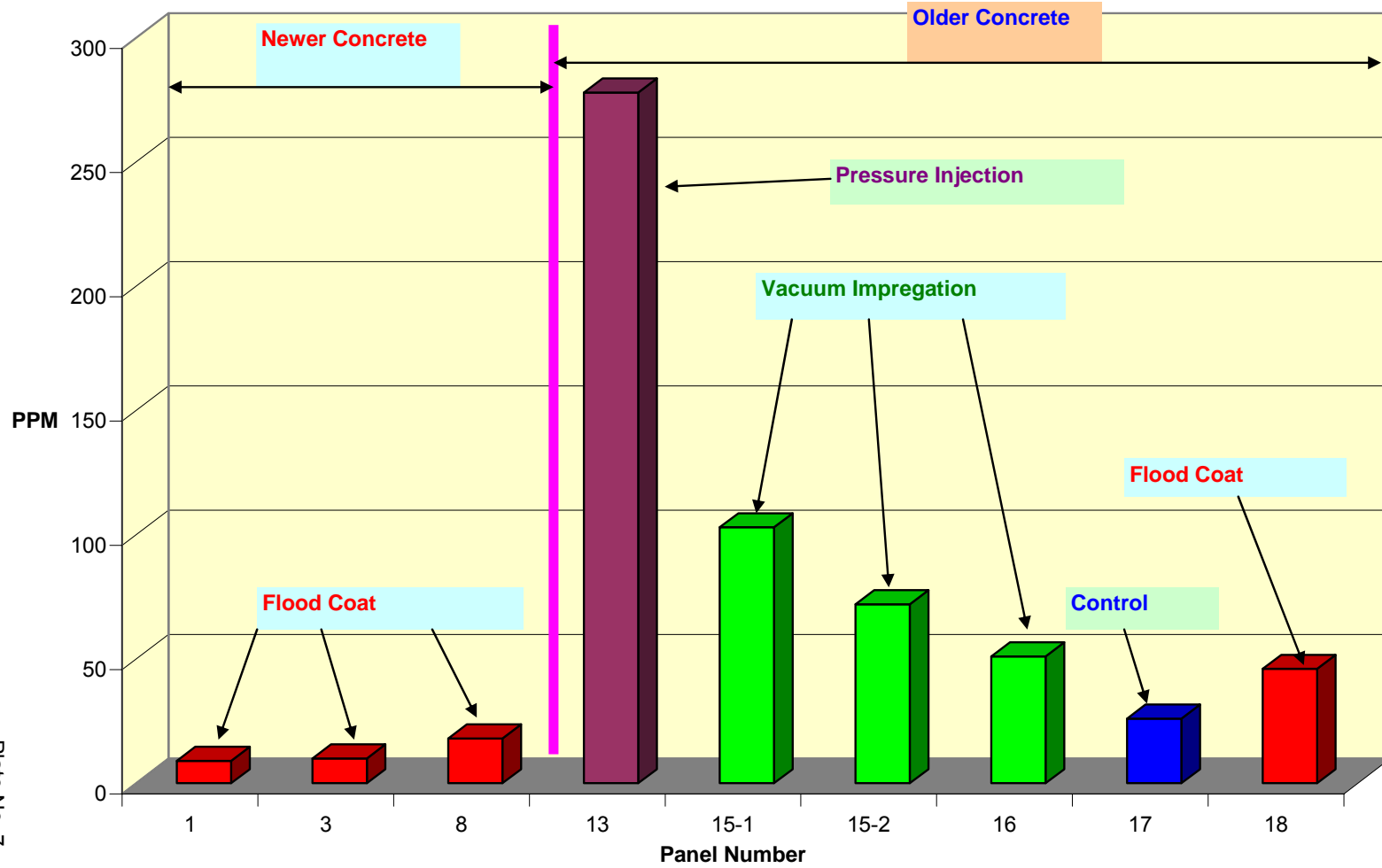


Plate No. 7

Average Lithium Content in Upper 4 Inches

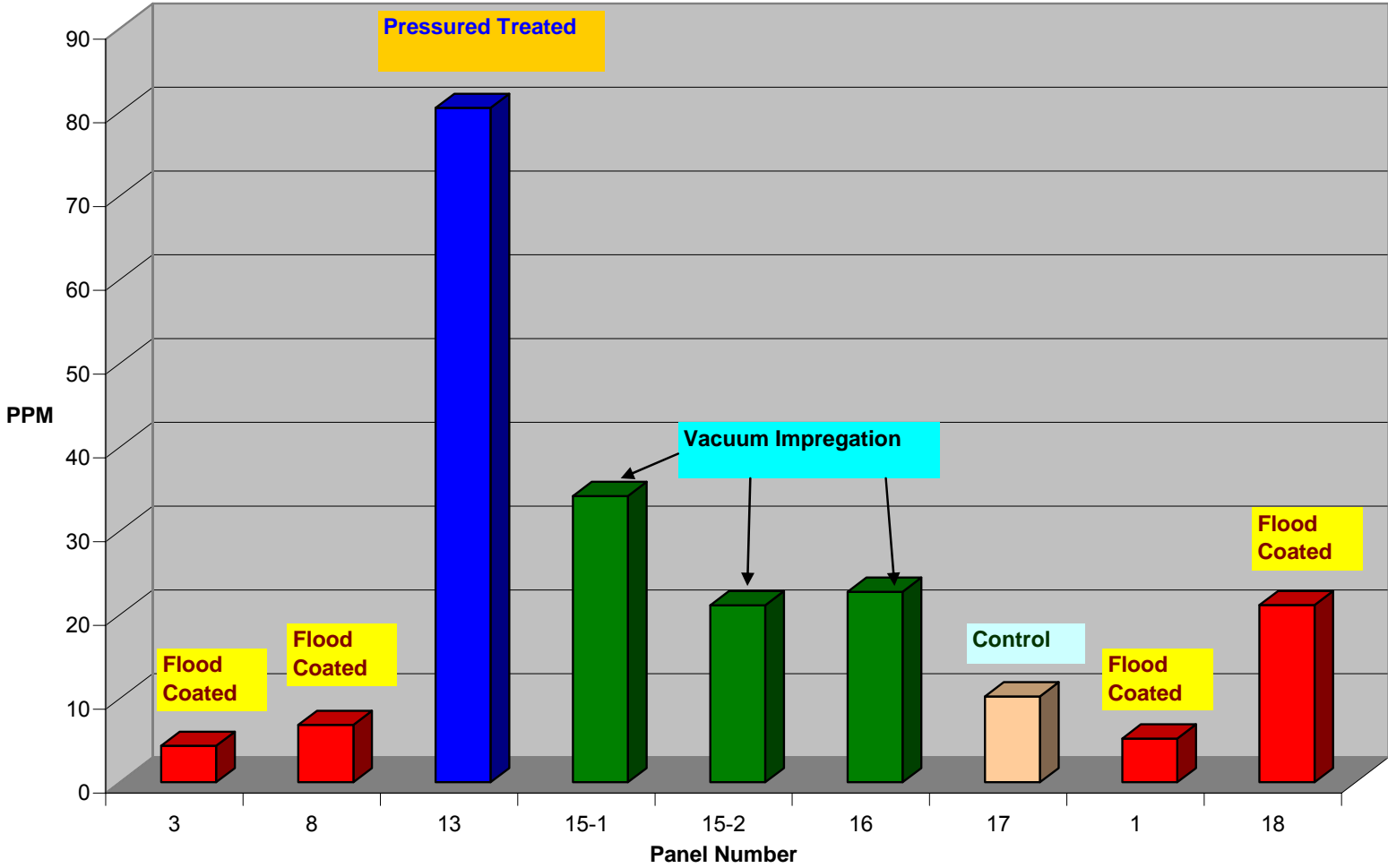


Plate No. 8